國立臺灣大學生命科學院生命科學系

碩士論文

Department of Life Science

College of Life Science

National Taiwan University

Master Thesis

狹口鏈渦蟲的負趨光行為

The Negative Phototactic Response in *Stenostomum grande*

陳建良

Jian-Liang Chen

指導教授：郭典翰 博士

Advisor: Dian-Han Kuo Ph. D.

中華民國 111 年 8 月

August, 2022

摘要

狹口鏈渦蟲 (*Stenostomum grande*) 是一種非寄生性的扁形動物，棲息於淡水環境。其身體結構十分簡單，且身上無明顯色素，且不具眼點。在大部分的動物當中，有色素的眼點可以用來感測光的方向，因此可以猜測缺乏眼點的狹口鏈渦蟲應該不具有方向性視覺。更令人驚訝的是，在鏈渦蟲的轉錄體資料庫中，並沒有找到動物界最常用來作為感光蛋白的視蛋白 (opsin) 及隱花色素 (cryptochrome)，這代表鏈渦蟲可能甚至沒有感光能力。然而在鏈渦蟲的行為實驗中，我們發現鏈渦蟲具有負趨光的行為反應，且這個行為反應具有光波長的專一性。對於短波長的可見光 (波長 454 nm 的藍光及 514 nm 的綠光)，傾向往光線來向的相反方向進行移動來躲避，且該反應的方向明確，並非透過隨機移動的方式抵達暗處，對長波長的光 (波長 594 nm 的黃光及 629 nm 的紅光) 則沒有特別的反應，即使被高強度的紅光雷射 (650 nm) 照射，也不會進行迴避。由於鏈渦蟲缺乏動物界常見的感光蛋白，但卻可對特定波長的光線產生行為反應，因此未來對鏈渦蟲感光機制的研究，將可進一步探索動物界裡感光機制的多樣性及演化可塑性。

關鍵字：狹口鏈渦蟲、光趨性、行為、光波長專一性

Abstract

Stenostomum grande is a free-living freshwater flatworm that has simple anatomy. It lacks pigmentation and has no apparent eyespot. An eyespot with a pigment screen is instrumental for sensing the direction of light in many animal species. Therefore, one might predict that *S. grande* cannot sense the directionality of light. Furthermore, transcripts encoding opsin and cryptochrome, the commonly used photosensory molecules in the animal kingdom, are missing from the transcriptome of *S. grande*. This would suggest that *S. grande* may not even have the ability to sense the light. However, we discovered that *S. grande* could respond to light and exhibit a negative phototaxis through behavioral experiments. Furthermore, the phototactic response of *S. grande* is spectrum-sensitive. *S. grande* exhibited negative phototactic behavior toward blue and green light (wavelength: 454 nm and 514 nm), and these worms would move to the dark side directly. However, *S. grande* is irresponsive to orange and red light (wavelength: 594 nm and 629 nm), even if the worms are exposed to a red laser ray with high intensity (650 nm). Given that this flatworm lacks the conventional photosensory molecules and yet exhibits a defined phototactic response, it is of great interest to further characterize the novel photosensory mechanism in this flatworm. Future studies of *Stenostomum* may shed light on the diversity and evolutionary plasticity of photosensory mechanisms in the animal kingdom.

Keywords: *Stenostomum*, phototaxis, behavior, spectral sensitivity
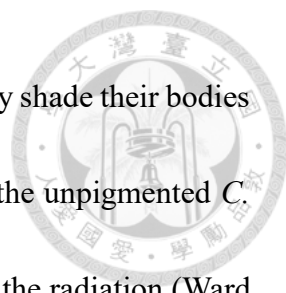
Content

Introduction

Light and Vision

For animals, it is essential to collect information from the environment and rapidly react to the stimuli to gain resources and avoid dangers.

Light is a medium that can deliver many different kinds of information. First, light carries visual information such as distance and properties of an object. Given the irrefutable advantage of vision, eyes evolved in various clades repeatedly. The most important function of vision is perceiving the direction of light. With this ability, animals can hide in a dark place from predators or move to a bright area to find resources. In addition to photoreceptor cells, pigment screens are also vital to detect the directionality of light (Jékely, 2009). Some animals have further evolved complex eyes to form spatial vision (Nilsson, 2009). With this complex eyes, animals can recognize the objects they see and visually communicate with others using colors, gestures, or movements. Furthermore, several clades have eyes with lens, which can form an inverted real image on the retina.

On the other hand, light may pose a danger to animals, especially short-wavelength light such as ultra-violet light (UV). UV can lead to DNA damage and cause mutation and cancer (Basu, 2018). Moreover, these rays with high energy would induce the production of reactive oxygen species that can damage the components of cells (Schuch

et al., 2017). In order to reduce the damage from UV, animals typically shade their bodies with melanin pigmentation and move away from UV. For example, the unpigmented *C. elegans* can sense the harmful UV light and try to avoid approaching the radiation (Ward et al., 2008).

In addition to the vision, animals also have nonvisual photoreceptor. In order to predict and adapt to the environmental changes associated with day-night transitions, animals would typically exhibit light-entrained circadian rhythms. Photoreceptors used to entrain the circadian rhythm, such as cryptochrome in *Drosophila* (Emery et al., 1998) and melanopsin in mammalian ipRGCs (Pickard and Sollars, 2011), differ from the opsins that are typically used for vision. Discriminating between day and night do not need to form directional light sensitivity, so the sensory organs can be simple. In conclusion, because light is a great medium to transmit information, it is common for animals to develop light sensing abilities.
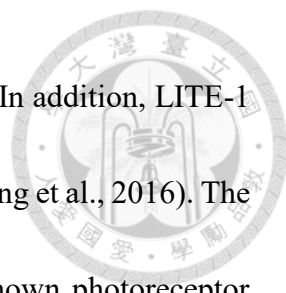
Photosensitive Molecules and Pigment Cells

Opsins are the universal photoreceptor proteins for vision in metazoans. Opsins, located in the membranous structure of photoreceptor cells such as the disks in vertebrate rods and cones, are seven-transmembrane molecules and belong to the G-protein-coupled receptors family (Terakita, 2005). Retinal, a chromophore derived from vitamin A, is

2

covalently linked to opsin and can absorb photons. After the light absorption, retinal

undergoes *cis-* to *trans-* transformation and activate the G-protein-coupled receptor

signaling pathway in the photoreceptor cells.

Cryptochrome is another photoreceptor protein in metazoans, although it was found

in plants in the beginning. The structure of cryptochromes is similar to photolyses, which

are photosensitive enzymes involved in DNA repair; therefore, it is believed that

cryptochromes were derived from photolyses but lost the ability of DNA repairing (Wang

et al., 2015). Cryptochromes are sensitive to short-wavelength light, such as UV light and

blue light. Cryptochromes, like opsins, require a chromophore, flavin adenine

dinucleotide (FAD), to absorb photons (Schwinn et al., 2020). Previous studies have

demonstrated that cryptochrome is involved in circadian clock (Damulewicz and

Mazzotta, 2020), phototactic responses (Rivera et al., 2012), and the sense of magnetic

field (Wiltschko et al., 2021).

Some metazoan species have lost opsins and cryptochromes, and yet they still can

respond to illumination. Take the nematode *C. elegans* as an example, researchers

observed the worms expressed strong aversion to near-UV light and blue light even

though the worms lack cerebral eyespots and known photosensitive molecules (Edwards

et al., 2008; Ward *et al.*, 2008). Several studies implicated that *C. elegans* uses a unique

protein to absorb short-wavelength light (Liu et al., 2010). Surprisingly, this 7

transmembrane protein, LITE-1, is a homolog of gustatory receptor. In addition, LITE-1 absorbs photons by itself without the assistance of chromophores (Gong et al., 2016). The features and mechanisms of LITE-1 are quite different from the known photoreceptor proteins in metazoans. These results imply the high plasticity of photoreceptor proteins and the possibility of the evolution of novel light absorption mechanisms in metazoans.

Animals can detect light by using their photoreceptor proteins; nonetheless, without a screening pigment, they may not perceive the direction of a light source (Jékely, 2009). Screen pigment in the eyespots has been implicated in the ability to sense the direction of light and is essential for phototactic behavior; moreover, these pigment cells can protect photoreceptors from damage by harmful light (Nilsson, 2009). Many clades of metazoans, such as Rotifer and Mollusca, respectively evolve a light sensing organ with similar pigment cells surrounding photoreceptors.

The Negative Phototactic Responses in Planarians

The eyes of planarians represent the simplest from vision. Due to the ability of rapid regeneration and well-developed genetic tools, planarians are popular for medical research. The anatomy of their nervous system (Kiyokazu Agata, 1998; Nakazawa, 2003) and their behavior (Elliott and Sánchez Alvarado, 2013) are well-described. Based on the experiments on planarian such as *Dugesia japonica* and *Schmidtea mediterranea*, the

details of the negative phototactic responses were observed and described (Parker and Burnett, 1900; Paskin et al., 2014; Taliaferro, 1920).
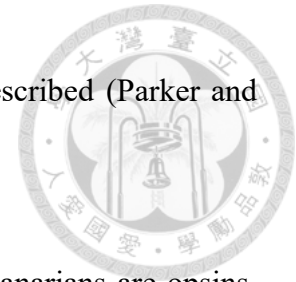
First, like other metazoans, the photosensitive molecules in planarians are opsins. Planarians are aversive to short-wavelength light (Paskin *et al.*, 2014), especially blue light (Shettigar et al., 2017). This phenomenon implicated that the absorption peak of opsins in planarians is about 475 nm. Besides visible light, the planarians also respond to UV. Nevertheless, the behavior in response to the exposure to UV differs from other kinds of visible light. The neuronal mechanism of visible light avoiding responses may not contribute to the flight from UV light (Shettigar et al., 2021). Rather, extraocular sensory network is responsible for generating the response to UV light. In addition, this network is independent from brain's control. The photoreceptor protein involved in extraocular sensory network is an opsins homolog.

Next, the photoreceptors and optic nerve can be marked by anti-arrestin antibody (Sakai et al., 2000). The pigment cells surround the photoreceptors and form a barrier to block light, which comes from particular directions, from reaching receptors. This structure plays a vital role in the negative phototactic response. Without this barrier, planarians could not recognize the direction of light (Akiyama et al., 2018). Furthermore, planarians would move with wigwag self-motions to collect more information of a light source. This phenomenon implicated that the mechanism to recognize where light comes

from is to differentiate the intensity of light in two eyespots. Therefore, data from the planarians demonstrate photoreceptor and pigment screen are both essential for phototactic response.

In conclusion, in order to generate a phototactic response, at least two structures are necessary: light absorptive molecules and a structure which can shade or refract light.

The Phylogenetic Position, Morphology, and Behavior of *S. grande*

Stenostomum grande is a member of Catenulida, the most basal lineage in Phylum Platyhelminthes (flatworms) (Laumer and Giribet, 2014). Due to its phylogenetic position, conducting research on this clade can help to reveal the evolutionary process leading to the flatworms and their relationship to other Spiralia clades.

S. grande is a small flatworm with simple morphology and anatomy (Noreña et al., 2005). *S. grande* reproduces asexually by paratomy. The reproductive process of *S. grande* differs from the one of Tricladida. For the species included in Tricladida, the fission behavior would be performed first, and then the fission fragment of planarian would develop into a complete organism (Malinowski et al., 2017). *S. grande*, however, generates several zooids at the posterior side. The zooids will not be separated until they are well developed as a mature organism (Rosa et al., 2015).

S. grande mainly swims in water propelled by the beating of epithelial cilia, and its

muscles are utilized to control the direction of movement. To put it another way, *S. grande* contracts its body wall until it makes a turn. *S. grande* can utilized dual gland adhesive organ to adhesive on a surface.

S. grande lives on the bottom of shallow freshwater. Without a great locomotive ability and special self-defense strategies, hiding in a narrow and dark place is the only way to survive. To increase the surviving rate, the worms have to develop some sensing abilities so that they can find a suitable living place. *S. grande* likes to stay at the wall and the corner of a breeding container. It seems that the worms can detect the properties of environment by sensation of touch and gravity. *S. grande* prefers to hide at a narrow place; hence the difficulty of experimental set-up.

The fact which *S. grande* is pale and semi-transparent indicates that it lacks pigmentation; indeed, it is apparent that it does not have eyespots (Fig. 1). Because of the importance of pigment cells to phototactic responses, *S. grande* was predicted not to exhibit phototaxis. Since phototaxis mediated by pigmented eyespots was found in both ingroup such as planarians and outgroup such as rotifers (Colangeli et al., 2019), the absence of pigmented eyes in *S. grande* is likely due to an evolutionary loss.

In this study, I performed a series of experiments to determine whether *S. grande* is able to exhibit phototactic responses without pigmented eye. The results demonstrate that *S. grande* can sense short-wavelength light and respond immediately. Future works on

the photosensory system in *Stenostomum* may reveal the diversity and evolutionary

plasticity of animal vision.

Material and Methods

Laboratory Culture of *S. grande*

The worms are cultured in a glass container. The worms live in artificial spring water (ASW) (0.032% sea salt in filtered tap water). The worms are fed with fish food or chicken liver 4~5 times a week. The water and container are changed once a week.

The Light Sources (LED Strips)

LED strips were used as the main light sources in most of the behavioral assays in this study. The wavelengths and intensities of the LEDs were measured by a luminometer, and the measuring was conducted 6.5 cm away from the light sources (Table 2, Fig. 2). Five different LED strips were white (Fig 2A), blue (Fig. 2B, peak = 454 nm), green (Fig. 2C, peak = 514 nm), orange (Fig. 2D, peak = 594 nm), and red (Fig 2E, peak = 629 nm). The LEDs were set with a 12 V power supplier, a switch, and a resistor which controls the intensities of lights. When conducting the assays, the LED strips were placed 6.5 cm away from the testing dish.

The Light Sources (Laser Rays)

Due to the high power of the laser rays, there is no instrument available for measuring their intensities and wavelengths. The specification of the laser rays was
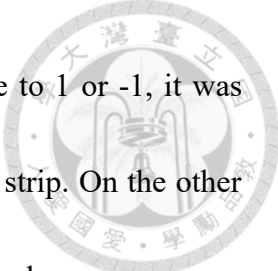
provided by the manufactures. Three laser rays were violet (405±10 nm) (max < 5 mW), green: (532 nm) (max < 10 mW), and red: (650±10 nm) (max < 5 mW). These rays were utilized in the laser irradiating test.
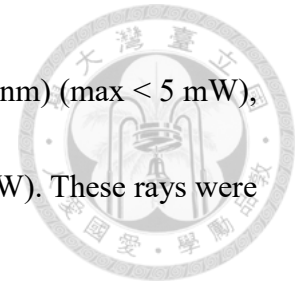
The Region Discrimination Assay and The Discrimination Index

The experimental setup is shown in Fig. 3A and 3B. A transparent plastic 90mm culture dish was divided into two regions: a dark region and a bright region. To reduce the reflection of light, the wall of the dark region was coated with black paint by using a marker pen. Given the unpigmented bodies of the worms, the lid and a black paper were stuck together to increase the contrast for better posture and movement recordings. To avoid image distortion caused by reflection, the camera (HP, Webcam w100) was mounted under the petri dish. A LED strip was set 6.5 cm away from the edge of the dish to produce a light gradient. To avoid the interference from ambient lighting, this assay was conducted in a dark room.

A group of 10 worms were put in the dish in each experiment, and 10 ml water was added. After 1 minute of illuminating, the numbers of worms in the bright region were recorded. The experiments of a group would be conducted 3 times to calculate the average, and five groups were used (n = 5, total 50 worms). The discrimination index was calculated by a formula: DI = (worms in the dark side – worms in the bright side) / total

10
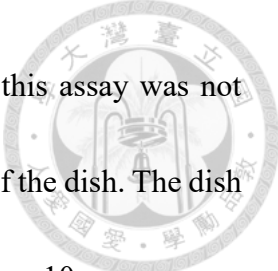
= (10 − 2 * (worms in the bright side)) / 10. If the DI value is close to 1 or -1, it was

interpreted as that the worms are repelled by or attracted to the LED strip. On the other

hand, if the DI value is close to 0, it was interpreted as that the worms show no response

to the light. The statistical significance was determined by one-way ANOVA and student's

t-test.

The Directional Phototactic Response Assay

In the same experimental setup shown in Fig. 3B and 3C, 30 worms were put in the

petri dish, and the movement was recorded by a camera. Five to ten worms were randomly

selected to perform the analysis of moving direction. The angles of the directions that the

head of the worm points to were record once per second, and 30 seconds of the

movements were recorded. ImageJ was utilized to measure the angles, and the polar charts

were made to visualize the directions of the movements. Percentages of data points in the

four quadrants relative to the light gradient were also plotted. The trajectories and the

speeds of the worms were also analyzed using ImageJ. The statistical significance of the

speeds was determined by one-way ANOVA.

The Wavelength Choosing Assay

Also in the same experimental setup, a blue and a green LED strips were placed on

the opposite sides of dish in this assay (Fig. 3D). The dish used in this assay was not

panted black, so lights from the two directions can penetrate the wall of the dish. The dish

was also divided into two regions: the green region and the blue region. 10 worms were

put in the testing dish and two lights were switched on at the same time (n = 3, total 30

worms). After 2 minute of illuminating, the numbers of worms in the blue region were

recorded. Three different light intensities were performed in this assay: blue : green = 1:1

(139.55 lux : 153 lux), blue : green = 1:2 (139.55 lux : 306 lux), and blue : green = 0.5:2

(69.78 lux : 306 lux). The discrimination index was calculated by a formula: DI = (worms

in the green side – worms in the blue side) / total = (10 – 2 * (worms in the blue side)) /

10. The statistical significance was determined by one-way ANOVA. The directional

analysis was conducted to characterize the moving patterns when the worms were

exposed to two opposing short-wavelength lights. the statistical analysis is the same as

previous ones.

The Laser Irradiating Test

A worm was placed in a dish, whose diameter was 60 mm culture dish, 5 ~ 7 ml of

water in it. This test was observed and recorded with camera mounted on an Olympus

SZX16 stereomicroscope in a dark room. The dark-field illumination with attenuated light

was used to provide homogenous ambient lighting for imaging. Because the worms tend

to stay at the corner or adhere on the wall, it was required to briefly shake the dish immediately before the test. When the test started, the worm would swim freely in the dish for 1 minute. Then the worm would be irradiated by a laser ray and the movement was recorded for 4 minutes. The distance from the laser pen to the surface of water was about 5 cm. The laser was aimed at a point roughly 2 mm anterior to the head of the worm. To avoid the influence of exhaustion, only the first five responses were collected and analyzed. Statistical test for the responses of worms toward lasers with different wavelengths were performed with *chi*-square test.

Identification of Specific Sequences

The target sequences (ChAT, IFT88, and arrestin) and candidate sequences (opsins, cryptochromes, BLUF photoreceptors, and LOV domain containing candidate sequences) were searched in the transcriptome database of *S. grande* with NCBI blast-2.12.0+.

Results

The Negative Phototactic Response in *S. grande*

In order to confirm whether *S. grande* can respond to a light gradient, a region discrimination assay was performed (Fig. 4A). In this experiment, illumination from a white-light LED strip was used to establish a linear light gradient. Worms were put in a petri dish which was divided into two regions: a bright region and a dark region (Fig. 4B, C). To block light from other directions, the wall of the dark region was painted with a black marker pen. After 60 seconds of illumination, the number of worms in each of the two regions was recorded separately. Then, the discrimination index (DI) of the test was calculated. The discrimination index was calculated by a formula: DI = (worms in the dark side – worms in the bright side) / total = (10 – 2 * (worms in the bright side)) / 10. The DI of white LED light is close to 1 (Fig. 4D), so it seems that the worms can sense the LED light and tend to stay in the dark.
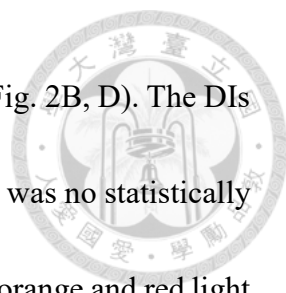
Two distinct mechanisms can explain the accumulation of worms in the dark after light exposure. First, the worms can only sense the existence of light. When they receive light exposure, their motility toward random direction increase. Once they arrived in the dark by chance, their motility decreases. Overtime, the number of worms would increase in the dark area. Next, the worms can detect the direction of the white light source with some unique mechanism. As a result, their movement would display an apparent

directionality toward the dark. To determine whether *S. grande* has a true phototactic

behavior, the movement of worms in the light gradient was recorded using a video camera.

In the control group, the worms were exposed to white light which was surrounded the

dish to eliminate the light gradient (Fig. 5A). In this setting, the worms changed their

moving directions frequently and did not move toward a specific direction (Fig. 5C, D,

H, I). However, when a light gradient was generated by directional illumination (Fig. 5B),

the worms moved away from the light source in 83.3% of the observation points (Fig. 5E,

F, G, J). Namely, the worms moved away from the white LED light. In short, these

experiments demonstrated that *S. grande* can detect the direction of white light and

exhibit negative phototaxis.

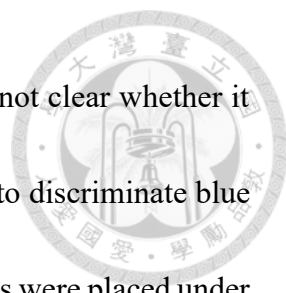**The Spectrum-Sensitive Phototactic Response**

A photoreceptor protein molecule typically responds to a specific range of light

spectrum. To determine whether the phototactic behavior of *S. grande* is spectrum-

sensitive, the worms were placed in light gradients with different spectral properties and

recorded for their movement. Single-color LED illumination was used as light source in

these experiment. The spectral properties of these LED light sources are: blue (peak =

454 nm), green (peak = 514 nm), orange (peak = 594 nm), and red light (peak = 629 nm)

(Table 2, Fig. 2). The phototactic assay was conducted in the same way as the region-

discrimination assay and the directional phototactic response assay (Fig. 2B, D). The DIs

of white, blue, and green light were all close to 1 (Fig. 4D), and there was no statistically

significant difference among these three groups. However, the DIs of orange and red light

were both close to 0, and there was a statistically significant difference between the DIs

between the responses to the long-wavelength light and short-wavelength light. This

result demonstrated that *S. grande* prefer to stay in the dark region when it is exposed to

short-wavelength light, but has no tendency to stay at a specific region in exposure to

long-wavelength light.

Similar to the regional discrimination assay, the worms exhibited different

movement pattern when exposed to light with different spectra in the phototaxis assay.

They move away from the light sources when irradiated with blue or green light (Fig. 6A,

B, 7A, B, 8A, B, 9A, B). On the other hand, when worms were exposed to orange or red

light, they moved toward random direction, typically circling (Fig. 6C, D, 7C, D, 8C, D,

9C, D). However, the speeds of movement were not significantly different among

different groups (Table 3), indicating that the observed phototactic response to light

constituted mostly by directional movement. In conclusion, the worms exhibit a negative

phototactic response to the blue and green light but not orange and red light.

Wavelength Discrimination

Although *S. grande* responds to both green and blue light, it is not clear whether it can distinguish the two colors. To determine the ability of *S. grande* to discriminate blue and green colors, a choosing assay was conducted. In this assay, worms were placed under opposing gradients of blue and green light and their movement patterns were recorded for analysis (Fig. 10A). If the worm exhibits a specific preference toward either the green or blue light, this would be indicative of the absorption peak in *S. grande*. When the worms were placed under opposing gradients of blue and green light with the same intensity (1:1). The discrimination index was about 0.5 (Fig. 10B) but their tracks of movement were more similar to that observed when worms were placed under flooded light or gradients of orange and red light (Fig. 11C). The head of the worm turned toward the source of green light in 43.33% of all observation points (Fig. 11A, B). These results indicated that the worms did not exhibit an apparent phototactic response, although they showed a weak preference to the green light.

To see if changing the ratio between intensities of blue and green light can the reverse the preference of green region, the intensity of green illumination over blue illumination, the worms were placed under opposing gradient of blue and green light, with an intensity ratio blue/green equaled 1/2 or 0.5/2, respectively. The averaged discrimination indexes were further reduced from the 1/1 experiments (Fig. 10B). Further, the moving trajectories were also similar to the 1:1 experiments. Therefore, the worms did not exhibit

a phototactic response in these experiments. This would suggest that *S. grande* does not significantly dislike blue illumination over green illumination or vice versa.
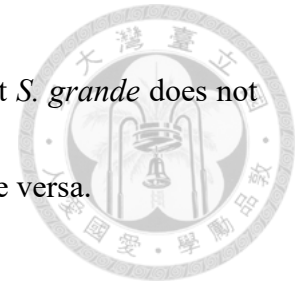
S. grande Behave Differently with Various Wavelength of Laser Rays

The phototactic response assays revealed that *S. grande* can detect short-wavelength light and move away from the light source. To see if this also applies to high-intensity light, a laser irradiating test was performed. Three different laser rays (violet: 404 nm, 5 mW; green: 539 nm, 10 mW; red: 664 nm, 5 mW) were utilized in these assays. In these tests, three categories of responses were defined as 1. "no response" if a worm goes through the lighted area without a pause; 2. "weak response" if a worm retracts after its head contact the light area; 3. "strong response" if a worm retracts before it comes across the lighted area.

Almost all the worms (94.74%) exhibited no response toward red laser (Fig. 12). About 69.2% of worms showed a weak response toward green laser. Most worms (82%) exhibited a strong response toward violet laser. Moreover, when a violet laser was aimed at a worm, it will contract its body and then escape. Therefore, despite the high-intensity of long-wavelength laser, *S. grande* does not respond to it at all, whereas it responds to short-wavelength laser. This is consistent with the results from the phototactic assays.
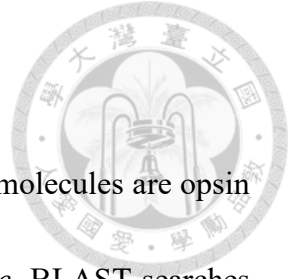
Missing Homologs of Photoreceptors

In the animal kingdom, the two commonly used photoreceptor molecules are opsin and cryptochrome. To find the potential photoreceptors in *S. grande*, BLAST searches were performed to identify the sequences of opsin and cryptochrome in the transcriptome databases of three different *Stenostomum* species, including *S. grande*, *S. leucops*, and *S. sthenum*. However, I found neither opsin nor cryptochrome in these transcriptomes. The best hit for opsin in these transcriptomes are neuropeptide receptors, as judged by reciprocal BLAST (Table 4). On the other hand, the best hit for cryotochrome is a small fragment that is nearly identical to a rotifer cryptochrome (Table 5). Since rotifers were food for *S. grande*, this is most likely a contamination.

Horizontal gene transfer is a way to get a new gene from other species (Keeling and Palmer, 2008). It is possible that *S. grande* expresses some unique genes which belong to prokaryotes. A sequence of BLUF photoreceptor (Jung et al., 2005), a photoreceptor protein which is mainly found in bacteria, from *Escherichia coli* and a sequence of LOV domain (Zoltowski et al., 2009) from *Arabidopsis thaliana* were used as query sequences, but the result was similar to the previous results (Table 6, 7). Ether fragmented sequence and low coverage or different protein sequences were found in the transcriptome database. In brief, it seems that *S. grande* may not have opsin, cryptochrome, and BLUF photoreceptor, which is from prokaryotes; thus, it may use some special ways to absorb

19

photons and recognize the direction of a light source.

Discussion

The Light-blocking Structure in *S. grande*

In Metazoa, pigmented eyespots are involved in vision. An eyespot typically consists of photoreceptor cells and pigment screen, which serves as a light barrier allowing only light from a certain direction to reach the photoreceptors. Without this barrier, however, the animals can only sense the existence of light, and cannot detect the direction of light, For most metazoans, the most prevalent strategy for forming a pigment screen is partial shading of their photoreceptors by pigment cells (Jékely, 2009; Nilsson, 2009). Nontheless, *Stenostomum grande* does not have eyespots with pigment cells, in spite of negative phototactic response it exhibiting. It is not clear how *S. grande* detects the direction of light. One possibility is that *S. grande* may adopt a unique barrier that is invisible to human eyes. For example, *C. elegans* also has phototaxis without eyespots, and the information of its barriers is still a puzzle (Ward *et al.*, 2008). In order to identify the position of the photoreceptor, it is important to study the neuroanatomy of *S. grande* (Appendix A).

The Short-wavelength-sensitive Response

After a series of assays, it is obvious that *S. grande* can respond to the graded blue and green lights, but not red and orange lights. Moreover, based on the laser irradiating test, despite the high intensity of red laser, the worms did not respond at all. Together,

these data suggest that *S. grande* can only sense short-wavelength visible light.

Each photoreceptor protein can be activated by light with a different ranges of light wavelength. In the wavelength choosing assay, the pattern of movement was similar to that when the worms were placed under a flooded light. It is possible that *S. grande* could not distinguish the blue and green light, implying that it may have only a single type of photoreceptor molecule. Yet, the worms still tended to stay away from blue light in the wavelength choosing assay. It is possible that the light absorption peak of this photoreceptor is closer to the region of blue light than the green light so that the opposing gradients of the blue and green light was perceived as a shallow light gradient by *Stenostomum*. To further test this hypothesis, it is necessary to identify the gene(s) encoding the photoreceptor proteins in *Stenostomum*.

The Unknown Photosensitive Molecules in *S. grande*

Opsin and cryptochrome are widely utilized by various metazoans as photoreceptor molecules. Because of the binding of chromophore, the functional domains of these two classes of proteins are conserved across species. However, transcripts encoding these conserved photoreceptors are missing from the transcriptomes of *Stenostomum*. Since opsins and cryptochromes were found in annelids, molluscs, and in other flatworms (Arendt, 2003; Oliveri et al., 2014), the absence of opsin and cryptochrome most likely

22

represents an evolutionary loss of these conserved photoreceptor genes in the lineage leading to *Stenostomum*.

To account for the phototactic behavior in *S. grande*, its ancestor must have evolved a novel photoreceptor. In one possibility a photosensitive molecule from other species may be laterally transferred into the genome of this hypothetical ancestor and used to sense light. Genes can be transferred by many vectors such as plasmid and virus (Keeling and Palmer, 2008), so it is possible that *S. grande* may possess bacterial photosensitive molecules. On the basis of my results from phototactic response assay, *S. grande* is sensitive to blue and green light. BLUF photoreceptors and LOV proteins are commonly used to sense short-wavelength light in bacteria and plants. However, I did not find a convincing homolog of these bacterial and plant photoreceptors in *Stenostomum* transcriptome. Therefore, the photoreceptor proteins may have evolved *de novo*.

Some non-opsin photoreceptors, such as LITE-1 in *C. elegans* and Gr28b in *Drosophila* larva body wall, are homologs of gustatory GPCRs (Gong *et al.*, 2016; Xiang et al., 2010). These photoreceptor proteins are different from opsins and cryptochromes because they do not use chromophores to absorb photons. In other words, they can sense light by using structures in the protein. Nevertheless, without a conserved chromophores binding domain, it is difficult to determine whether the candidate sequences are photosensitive. The only way to ascertain the function of the candidate sequences is

performing loss-of-function experiments with genetic tools; therefore, RNAi with dsRNA

was tried (Appendix B).

Appendix A. The Nervous Anatomy of *S. grande*

Material and Methods

<u>DNA cloning and plasmid preparation</u>

The mRNAs of the worms were extracted by Direct-zol RNA MiniPrep Kit (Zymo Research). The cDNA sequences were synthesized by reverse transcription. The target cDNA sequences were amplified by Taq PCR 2X Master mix (MDbio) and phusion (Thermo). The used primers are listed in Table 1. After electrophoresis with 1% agarose gel, the target cDNA sequences were purified by Zymoclean Gel DNA Recovery Kit (Zymo Research). These sequences were inserted into pCRII vector (Invitrogen) by T4 ligase (ThermoFisher). The vectors were sent into DH5α *E. coli* by heat shock, a method to conduct transformation. The transformed bacteria were cultured on the LB plates containing ampicillin (MDbio), X-Gal (MDbio), and β-d-1-thiogalactopyranoside (IPTG) at 37℃ for 16 hours. Only white colonies were selected and culture in liquid at 37℃ for 16 hours. Plasmids were extracted by ZR Plasmid Miniprep Classic (Zymo Research).

<u>The preparation of probes</u>
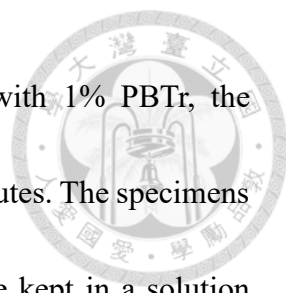
The DNA templates of ChAT were produced by Taq PCR 2X Master mix (MDbio) and M13 forward and reverse primers. Then the templates were purified by DNA Clean & Concentrator (Zymo Research). Digoxigenin-labeled RNA probes were synthesized

with SP6 RNA polymerase (ThermoFisher). The reaction was incubated at 37 ℃ for at least 4 hours. After the synthesis, 1 μl of RNase-free DNase was added and incubate at 37 ℃ for 30 minutes. The next procedure was RNA precipitation with ethanol. First, 4 μl 6M lithium chloride was added. Then 100 μl cold 100% EtOH was added and the liquid was mixed well. The mixture was stored at -20 ℃ for at least 1 hour. The mixture was centrifuged at maximal speed (13000 rcf) at 4 ℃ for 15 minutes to pellet the RNA probe. The pellet was washed with cold 75% EtOH and was centrifuged at maximal speed (>13000 rcf) at room temperature for 5 minutes. The pellet was air-dried for 5 minutes. The pellet was resuspended in 15 μl RNase-free water. The concentration of RNA was measured by NanoDrop One (Thermo). Finally, the probes were diluted with prehybridization buffer (PreHyb), and the final concentration was 200 ng/μl.

Whole-mount *in situ* hybridization

Before *in situ* hybridization and immunostaining, the worms had to be starved for at least 2 days to empty their guts. Specimens were prefixed briefly in 100% methanol. After the prefixation, methanol was replaced with 4% paraformaldehyde (PFA) in PBS. The specimens were fixed at room temperature for 1 hour. After the fixation, the specimens were washed with PBS supplemented with 1% Triton X-100 (PBTr) five times briefly. 0.125 μl proteinase K was added in 500 μl 1% PBTr and the specimens were kept in the

liquid at room temperature for 10 minutes. After a short wash with 1% PBTr, the specimens were postfixed in 4% PFA at room temperature for 30 minutes. The specimens were washed with 1% PBTr five times briefly. The specimens were kept in a solution which was mixed with 250 μl 1% PBTr and 250 μl PreHyb at 60 °C for 10 minutes. The solution was replaced with 500 μl PreHyb, and the specimens were incubated at 60 °C overnight. The next day, 1 μl riboprobe (*ChAT*) were added in 300 μl PreHyb and kept incubating at 60 °C overnight. After hybridization, the specimens were washed with a 1:1 mixture of PreHyb & 2X SSC at 60 °C for 20 minutes. The wash was continued with three 2X SSC washes, four 0.2X SSC washes, and two 0.1X SSC washes. Each wash was carried out at 60 °C and lasted for 20 minutes. Then the specimens were washed by 1% PBTr at room temperature with gentle rocking for 10 minutes. The specimens were kept in 500 μl anti-dig blocking solution at RT with gentle rocking for 3 hours. 0.2 μl sheep α dig-AP was added, and the specimens were gently rocked at 4 °C overnight. After applying the antibody, the worms were washed 6 times by 1% PBTr at RT with gentle rocking for 20 minutes. The specimens were kept in filtered AP buffer twice for 5 minutes. When color development, 4 μl NBT and 1 μl BCIP were added in 250 μl AP buffer. The specimens were incubated at 37 °C for about 2 hours. The specimens were washed by 1% PBTr three times with gentle rocking for 10 minutes. To reveal the positions of nuclei, the specimens were incubated in a solution with 500 μl 1% PBTr and 0.5 μl Hoechst
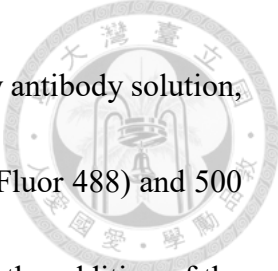
33342 at room temperature for 30 minutes. Then the specimens were stored in 70%

glycerol at 4 ˚C.

Immunostaining

To relax the muscles, specimens were put in a solution which was prepared by a mix

of 500 μl ASW and 250 μl 0.25M MgCl₂. After a few seconds of relaxation, the solution

containing MgCl₂ was replaced with 200 μl 4% PFA in 2.5X PBS. The specimens were

fixed at room temperature for 1 hour. After the fixation, the specimens were washed with

1% PBTr once with gentle rocking for 10 minutes. Then the specimens were washed with

1% PBTr 4 times briefly. 0.125 μl proteinase K was added in 500 μl 1% PBTr and the

specimens were kept in the liquid at room temperature for 10 minutes. Then the specimens

were washed with 1% PBTr twice with gentle rocking for 10 minutes.

The specimens were kept in 500 μl 5% blocking solution at 4 ˚C with gently rocking

overnight. The 5% blocking solution was prepared by mixing 5 ml WBS, 2.5 ml NGS,

0.5 ml Triton X-100, and filled up with 1X PBS. On the next day, the blocking solution

was replaced with a new one, and the primary antibodies were added (rabbit anti-

FMRFamide, Immunostar, 2μl; rabbit anti-planarian arrestin, Lagen, 1 μl). The specimens

were incubated in the primary antibody solution at 4 ˚C with gently rocking overnight.

After the incubation, the specimens were washed with 1% PBTr 6 times with gentle

28
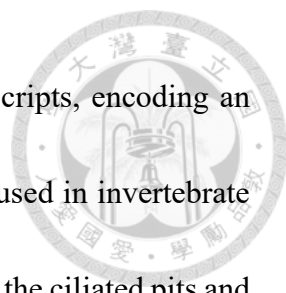
rocking for 15 minutes. The specimens were incubated in a secondary antibody solution, which was consist of 1 μl secondary antibody (goat anti-rabbit AlexaFluor 488) and 500 μl 5% blocking solution, at 4 ˚C with gently rocking overnight. After the addition of the secondary antibody, the specimens were covered with aluminum foil to block external light. The specimens were washed with 1% PBTr 6 times with gentle rocking for 15 minutes after the incubation. The specimens were incubated in a solution with 500 μl 1% PBTr and 0.5 μl Hoechst 33342 at room temperature for 30 minutes. Then the specimens were stored in 70% glycerol at 4 ˚C.

Microscope observation

The specimens of immunostaining and WISH were mounted on a microscope slide. To keep the specimens from crushing between the slide glass and the coverslip, two plastic binder reinforcement rings were utilized to form a space. The photos were taken by an Olympus DP80 CCD camera mounted on an automated Olympus BX63 microscope.

Results

In addition to a photoreceptor, animal phototaxis behavior also requires a nervous system. Little is known about the organization of nervous system in *Stenostomum*. To identify the neurons involved in motor control in *Stenostomum*, whole-mount in situ

hybridization (WISH) to the choline acetyltransferase (ChAT) transcripts, encoding an enzyme that synthesize acetylcholine, neurontransmitter commonly used in invertebrate motor neurons (Turner et al., 2013). Four small clusters of cell behind the ciliated pits and a few scattered cells posterior to the pharynx were found to express ChAT transcript (Fig. 13). At the dorsal side of the trunk, additional four cell clusters were posterior to each fission plan. These cells may be the developing motor neurons in the zooids.

FMRFamide-like peptides, are involved in many kinds of animal behavior (Day and Maule, 1999; Gustafsson et al., 2002). In *Stenostomum*, FMRFamide-like immunoreactive (-lir) cells and fibers can be found in several regions (Fig. 14) (Reuter et al., 2001; Wikgren and Reuter, 1985). In the head FMRFamide-ergic cells were located in the cerebral ganglion behind ciliated pits. Similarly configured FMRFamide-lir cells are found posterior to the fission plan. FMRFamide-lir fibers can be seen on the ventral side of trunk and around the pharynx. At the ventral side, four longitudinal nerves are found.

Discussion

Flatworms possess orthogonal nervous system. Several main longitudinal nerves connect their brain and caudal region, and many connecting commissures can transmit signals from one longitudinal nerve to another (Reuter et al., 1995). It is hypothesized

that species in Catenulida may also have the same features.

The structure of nervous system in *Stenotomum* has been revealed for years. For example, FMRFamide-like immunoreactive nerve cords can only be observed at the ventral side, and the FMRFamide-like immunoreactive pharyngeal nerve ring was suggested to control pharynx muscles (Reuter *et al.*, 2001; Wikgren and Reuter, 1985) (Fig. 14).

In order to reveal the center of motor control, the cell bodies which express ChAT are revealed by WISH. Astonishingly, the cell bodies are located in the cerebral ganglion and around the pharynx. The distribution of the ChAT signals is similar to the FMRFamide signals except the longitudinal nerves. This result demonstrated that the signals of external stimuli may send to the cerebral ganglion, and the center of motor control will produce neurotransmitters and send the signals to muscles by longitudinal nerves.
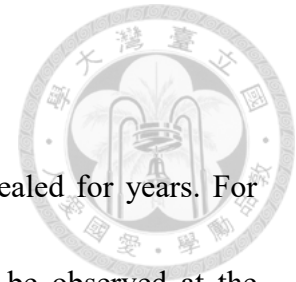
Appendix B. Validation of Feeding dsRNA in *S. grande*

Material and Methods

The preparation of dsRNA

The DNA templates for dsRNA synthesis were prepared as described for probe synthesis. SP6 RNA polymerase (ThermoFisher) and T7 RNA polymerase (ThermoFisher) were used to synthesized the sense and antisense RNA from unlabeled NTPs. The dsRNA was diluted with ddH$_2$O to a final concentration of 1000 ng/µl.

Performing RNA interference by feeding dsRNA

Before dsRNA feeding, about 100 worms were starved for at least two days. The feeding regime lasted 7 days, and the worms were fed every other day. The dsRNA-containing food was made by mixing 6 µl dsRNA, 12 µl chicken liver, and 6 µl 2% low melting agarose (or in the same ratio for other volume). After the mix, the food was stored at -20 °C for 5 minutes and was used immediately. To identify the worms eating the dsRNA-containing foods, 0.5 µl Fast-Green dye was added in the food. In 2 hours after the final feeding, the worms were transferred into a new container. The worms were distributed into three groups, each containing 20 worms. The RNA of the worms were extracted by Direct-zol RNA MiniPrep Kit (Zymo Research) after 4 hours. First-strand cDNA sequences were then synthesized by reverse transcription.

Quantitative real time PCR

To analyzed the expression level of target genes in each dsRNA-feeding group,

quantitative real time PCR (qPCR) was performed by using qPCR thermocycler (CFX

Connect Real-Time PCR Detection System, Bio-Rad). The reactions were conducted with

biological replication (60 worms from one feeding treatment were separated into 3 groups)

and technical replication (the same reaction of each group would be conducted 3 times).

Each tube of reaction contained 10 µl SYBR green supermix, 0.5 µl 10 µM forward primer,

0.5 µl 10 µM reverse primer, 1 µl cDNA, and 8 µl ddH$_2$O (total = 20 µl). The primers

used are listed in Table 1. The expression levels were conducted by comparison with β-

actin expression. The statistical significance was determined by student's t test.

Results

In planarians, RNA interference by feeding double-strandeds RNA (dsRNA) to the

animal is a useful way for characterize gene functions (Rouhana et al., 2013). To

determine if feeding dsRNA is also useful in *Stenostomum*, dsRNA corresponding to

fragments of *Sg-Arrestin*, encoding a G protein coupled receptor associated protein, *Sg-*

IFT88, encoding a ciliary component, and Sg-*ChAT,* and GFP control were fed to the

worm. The levels of gene knockdown were assayed by qPCR was conducted. The results

showed that the expression levels of the genes of interest decreased by ~19% to ~43% (Fig. 15A, B, C). Nonetheless, only ds*Arr* RNAi results in a significant difference to the control (Fig. 15D, E, F). It seems that RNAi by feeding dsRNA may not be consistently effective .in S. grande.

Discussion

Feeding dsRNA is a common way to knock down target genes in the planarian. dsRNA can be mixed with food (liver paste), water, and dye, and the dsRNA will be absorbed by the worms (Rouhana *et al.*, 2013). In my dsRNA feeding experiments, expression levels of three testing groups were all dropped in *S. grande*. My results implicated that feeding dsRNA may be a way to decrease the expression of target genes. However, no phenotypic change was observed. It is possible that the efficacies of gene knockdown were not sufficient to result in visible loss-of-function phenotypes in these experiments.

References

Akiyama, Y., Agata, K., and Inoue, T. (2018). Coordination between binocular field and spontaneous self-motion specifies the efficiency of planarians' photo-response orientation behavior. *Communications Biology 1*. doi: 10.1038/s42003-018-0151-2.

Arendt, D. (2003). Evolution of eyes and photoreceptor cell types. *International Journal of Developmental Biology 47*, 563-571.

Basu, A. (2018). DNA Damage, Mutagenesis and Cancer. *International Journal of Molecular Sciences 19*, 970. doi: 10.3390/ijms19040970.

Colangeli, P., Schlägel, U.E., Obertegger, U., Petermann, J.S., Tiedemann, R., and Weithoff, G. (2019). Negative phototactic response to UVR in three cosmopolitan rotifers: a video analysis approach. *Hydrobiologia 844*, 43-54. doi: 10.1007/s10750-018-3801-y.

Damulewicz, M., and Mazzotta, G.M. (2020). One Actor, Multiple Roles: The Performances of Cryptochrome in *Drosophila*. *Frontiers in Physiology 11*, 99. doi: 10.3389/fphys.2020.00099.

Day, T.A., and Maule, A.G. (1999). Parasitic peptides! The structure and function of neuropeptides in parasitic worms. *Peptides 20*, 999-1019. doi: 10.1016/s0196-9781(99)00093-5.

Edwards, S.L., Charlie, N.K., Milfort, M.C., Brown, B.S., Gravlin, C.N., Knecht, J.E.,

and Miller, K.G. (2008). A Novel Molecular Solution for Ultraviolet Light Detection in *Caenorhabditis elegans*. *PLoS Biology 6*, e198. doi: 10.1371/journal.pbio.0060198.

Elliott, S.A., and Sánchez Alvarado, A. (2013). The history and enduring contributions of planarians to the study of animal regeneration. *Wiley Interdisciplinary Reviews: Developmental Biology 2*, 301-326. doi: 10.1002/wdev.82.

Emery, P., So, W.V., Kaneko, M., Hall, J.C., and Rosbash, M. (1998). CRY, a *Drosophila* Clock and Light-Regulated Cryptochrome, Is a Major Contributor to Circadian Rhythm Resetting and Photosensitivity. *Cell 95*, 669-679. doi: 10.1016/s0092-8674(00)81637-2.

Gong, J., Yuan, Y., Ward, A., Kang, L., Zhang, B., Wu, Z., Peng, J., Feng, Z., Liu, J., and Xu, X.Z.S. (2016). The *C. elegans* Taste Receptor Homolog LITE-1 Is a Photoreceptor. *Cell 167*, 1252-1263.e1210. doi: 10.1016/j.cell.2016.10.053.

Gustafsson, M.K.S., Halton, D.W., Kreshchenko, N.D., Movsessian, S.O., Raikova, O.I., Reuter, M., and Terenina, N.B. (2002). Neuropeptides in flatworms. *Peptides 23*, 2053-2061, Pii s0196-9781(02)00193-6. doi: 10.1016/s0196-9781(02)00193-6.

Jékely, G. (2009). Evolution of phototaxis. *Philosophical Transactions of the Royal Society B: Biological Sciences 364*, 2795-2808. doi: 10.1098/rstb.2009.0072.

Jung, A., Domratcheva, T., Tarutina, M., Wu, Q., Ko, W.H., Shoeman, R.L., Gomelsky,

M., Gardner, K.H., and Schlichting, L. (2005). Structure of a bacterial BLUF photoreceptor: Insights into blue light-mediated signal transduction. *Proceedings of the National Academy of Sciences of the United States of America 102*, 12350-12355. doi: 10.1073/pnas.0500722102.

Keeling, P.J., and Palmer, J.D. (2008). Horizontal gene transfer in eukaryotic evolution. *Nature Reviews Genetics 9*, 605-618. doi: 10.1038/nrg2386.

Kiyokazu Agata, Y.S., Kentaro Kato, Chiyoko Kobayashi, Yoshihiko Umesono, Kenji Watanabe (1998). Structure of the Planarian Central Nervous System (CNS) Revealed by Neuronal Cell Markers. *Zoological Science 15,* 433-440. doi: 10.2108/zsj.15.433

Laumer, C.E., and Giribet, G. (2014). Inclusive taxon sampling suggests a single, stepwise origin of ectolecithality in Platyhelminthes. *Biological Journal of the Linnean Society 111*, 570-588. doi: 10.1111/bij.12236.

Liu, J., Ward, A., Gao, J., Dong, Y., Nishio, N., Inada, H., Kang, L., Yu, Y., Ma, D., Xu, T., et al. (2010). *C. elegans* phototransduction requires a G protein–dependent cGMP pathway and a taste receptor homolog. *Nature Neuroscience 13*, 715-722. doi: 10.1038/nn.2540.

Malinowski, P.T., Cochet-Escartin, O., Kaj, K.J., Ronan, E., Groisman, A., Diamond, P.H., and Collins, E.M.S. (2017). Mechanics dictate where and how freshwater

planarians fission. *Proceedings of the National Academy of Sciences of the United States of America 114*, 10888-10893. doi: 10.1073/pnas.1700762114.

Nakazawa, M. (2003). Search for the Evolutionary Origin of a Brain: Planarian Brain Characterized by Microarray. *Molecular Biology and Evolution 20*, 784-791. doi: 10.1093/molbev/msg086.

Nilsson, D.-E. (2009). The evolution of eyes and visually guided behaviour. *Philosophical Transactions of the Royal Society B: Biological Sciences 364*, 2833-2847. doi: 10.1098/rstb.2009.0083.

Noreña, C., Damborenea, C., and Brusa, F. (2005). A taxonomic revision of South American species of the genus *Stenostomum* O. Schmidt (Platyhelminthes: Catenulida) based on morphological characters. *Zoological Journal of the Linnean Society 144*, 37-58. doi: 10.1111/j.1096-3642.2005.00157.x.

Oliveri, P., Fortunato, A.E., Petrone, L., Ishikawa-Fujiwara, T., Kobayashi, Y., Todo, T., Antonova, O., Arboleda, E., Zantke, J., Tessmar-Raible, K., and Falciatore, A. (2014). The Cryptochrome/Photolyase Family in aquatic organisms. *Marine Genomics 14*, 23-37. doi: 10.1016/j.margen.2014.02.001.

Parker, G.H., and Burnett, F.L. (1900). The reactions of planarians, with and without eyes, to light. *American Journal of Physiology-Legacy Content 4*, 373-385.

Paskin, T.R., Jellies, J., Bacher, J., and Beane, W.S. (2014). Planarian Phototactic Assay
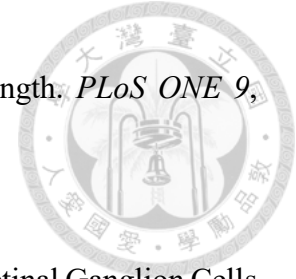
Reveals Differential Behavioral Responses Based on Wavelength. *PLoS ONE 9*, e114708. doi: 10.1371/journal.pone.0114708.

Pickard, G.E., and Sollars, P.J. (2011). Intrinsically Photosensitive Retinal Ganglion Cells. *Reviews of Physiology, Biochemistry and Pharmacology*, 59-90. doi: 10.1007/112_2011_4.

Reuter, M., Gustafsson, M.K.S., Sheiman, I.M., Terenina, N., Halton, D.W., Maule, A.G., and Shaw, C. (1995). The nervous system of Tricladida. II. Neuroanatomy of *Dugesia tigrina* (Paludicola, Dugesiidae): An immunocytochemical study. *Invertebrate Neuroscience 1*, 133-143. doi: 10.1007/bf02331911.

Reuter, M., Raikova, O.I., and Gustafsson, M.K.S. (2001). Patterns in the nervous and muscle systems in lower flatworms. *Belgian Journal of Zoology 131*, 47-53.

Rivera, A.S., Ozturk, N., Fahey, B., Plachetzki, D.C., Degnan, B.M., Sancar, A., and Oakley, T.H. (2012). Blue-light-receptive cryptochrome is expressed in a sponge eye lacking neurons and opsin. *Journal of Experimental Biology 215*, 1278-1286. doi: 10.1242/jeb.067140.

Rosa, M.T., Pereira, C.M., Ragagnin, G.T., and Loreto, E.L.S. (2015). *STENOSTOMUM LEUCOPS* DUGÈS, 1828 (PLATYHELMINTHES, CATENULIDA): A PUTATIVE SPECIES COMPLEX WITH PHENOTYPIC PLASTICITY. *Papéis Avulsos de Zoologia (São Paulo) 55*, 375-383. doi: 10.1590/0031-1049.2015.55.27.
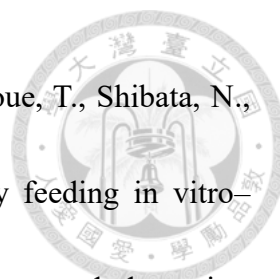
Rouhana, L., Weiss, J.A., Forsthoefel, D.J., Lee, H., King, R.S., Inoue, T., Shibata, N., Agata, K., and Newmark, P.A. (2013). RNA interference by feeding in vitro–synthesized double-stranded RNA to planarians: Methodology and dynamics. *Developmental Dynamics 242*, 718-730. doi: 10.1002/dvdy.23950.

Sakai, F., Agata, K., Orii, H., and Watanabe, K. (2000). Organization and Regeneration Ability of Spontaneous Supernumerary Eyes in Planarians —Eye Regeneration Field and Pathway Selection by Optic Nerves—. *Zoological Science 17*, 375-381. doi: 10.2108/jsz.17.375.

Schuch, A.P., Moreno, N.C., Schuch, N.J., Martins Menck, C.F., and Machado Garcia, C.C. (2017). Sunlight damage to cellular DNA: Focus on oxidatively generated lesions. *Free Radical Biology and Medicine 107*, 110-124. doi: 10.1016/j.freeradbiomed.2017.01.029.

Schwinn, K., Ferré, N., and Huix-Rotllant, M. (2020). UV-visible absorption spectrum of FAD and its reduced forms embedded in a cryptochrome protein. *Physical Chemistry Chemical Physics 22*, 12447-12455. doi: 10.1039/d0cp01714k.

Shettigar, N., Chakravarthy, A., Umashankar, S., Lakshmanan, V., Palakodeti, D., and Gulyani, A. (2021). Discovery of a body-wide photosensory array that matures in an adult-like animal and mediates eye–brain-independent movement and arousal. *Proceedings of the National Academy of Sciences 118*, e2021426118. doi:
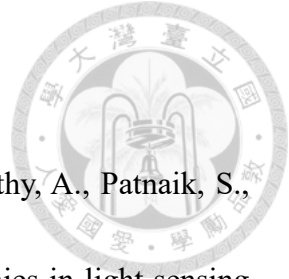
10.1073/pnas.2021426118.

Shettigar, N., Joshi, A., Dalmeida, R., Gopalkrishna, R., Chakravarthy, A., Patnaik, S., Mathew, M., Palakodeti, D., and Gulyani, A. (2017). Hierarchies in light sensing and dynamic interactions between ocular and extraocular sensory networks in a flatworm. *Science Advances 3*, e1603025. doi: 10.1126/sciadv.1603025.

Taliaferro, W.H. (1920). Reactions to light in Planaria maculata, with special reference to the function and structure of the eyes. *Journal of Experimental Zoology 31*, 58-116. doi: 10.1002/jez.1400310103.

Terakita, A. (2005). The opsins. Genome Biology *6*, 213. 10.1186/gb-2005-6-3-213.

Turner, J.R., Gold, A., Schnoll, R., and Blendy, J.A. (2013). Translational Research in Nicotine Dependence. *Cold Spring Harbor Perspectives in Medicine 3*, a012153-a012153. doi: 10.1101/cshperspect.a012153.

Wang, J., Du, X.L., Pan, W.S., Wang, X.J., and Wu, W.J. (2015). Photoactivation of the cryptochrome/photolyase superfamily. *Journal of Photochemistry and Photobiology C-Photochemistry Reviews 22*, 84-102. doi: 10.1016/j.jphotochemrev.2014.12.001.

Ward, A., Liu, J., Feng, Z., and Xu, X.Z.S. (2008). Light-sensitive neurons and channels mediate phototaxis in C. elegans. *Nature Neuroscience 11*, 916-922. doi: 10.1038/nn.2155.

Wikgren, M.C., and Reuter, M. (1985). NEUROPEPTIDES IN A MICROTURBELLARIAN - WHOLE MOUNT IMMUNOCYTOCHEMISTRY. *Peptides 6*, 471-475. doi: 10.1016/0196-9781(85)90416-4.

Wiltschko, R., Niessner, C., and Wiltschko, W. (2021). The Magnetic Compass of Birds: The Role of Cryptochrome. *Frontiers in Physiology 12*, 667000. doi: 10.3389/fphys.2021.667000.

Xiang, Y., Yuan, Q., Vogt, N., Looger, L.L., Jan, L.Y., and Jan, Y.N. (2010). Light-avoidance-mediating photoreceptors tile the Drosophila larval body wall. *Nature 468*, 921-926. doi: 10.1038/nature09576.

Zoltowski, B.D., Vaccaro, B., and Crane, B.R. (2009). Mechanism-based tuning of a LOV domain photoreceptor. *Nature Chemical Biology 5*, 827-834. doi: 10.1038/nchembio.210.

Tables and Figures
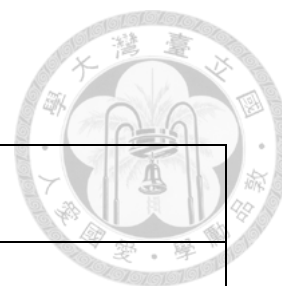
Table 1 Primers used in the experiments

Primer name	Sequence
*ChAT*_probe_forward	TCGATTCGGGCGTGATTTTC
*ChAT*_probe_reverse	GGCCTGATAACTTCTGCAGC
*ChAT*_dsRNA_forward	TCGCCTCTTCACGTCCTATC
*ChAT*_dsRNA_reverse	CACGTCGTCCTCACTCAAAC
*ChAT*_qPCR_forward	CCGCTACGAGGCGTTAGTGA
*ChAT*_qPCR_reverse	ACCTGCCACCAACCTAGCAG
*IFT88*_dsRNA_forward	CAAACGTCACTGCATGGTCA
*IFT88*_dsRNA_reverse	CACTGGTTTCTGCCGTTTGA
*IFT88*_qPCR_forward	TGGTGAACCGAGGTAACGTG
*IFT88*_qPCR_reverse	AGTTCGTGAATGACGGCGAT
*Arr*_dsRNA_forward	TCCCGATTCATCCCAACCAA
*Arr*_dsRNA_reverse	AATACAGGCGCACTTTGACG
*Arr*_qPCR_forward	ATTCGGCAATGGTGACCTGT
*Arr*_qPCR_reverse	GCTGTCTGCTCTGTTCGACT

43

Table 2 The LED light intensities used in the phototactic response assay

Light	Intensity (lux)	PPFD (μmol /m²/s)	PFD-B (μmol /m²/s)	PFD-G (μmol /m²/s)	PFD-R (μmol /m²/s)
white	580.681417	7.95094	2.14312	3.97498	1.66864
blue	139.5474903	12.1657	11.8531	0.17492	0.05959
green	458.996745	4.79768	0.78299	4.00289	0.01179
red	318.932261	8.16012	0.06426	0.2676	7.66287
orange	399.94103	4.34406	0.03189	2.84377	1.38599

Table 3 The mean speeds in different testing groups (n = 5 in each group)

Group	Mean speed (mm/s)	Standard deviation
control 1	1.371655951	0.499081396
control 2	1.337025489	0.183520973
white	1.955136199	0.808064708
blue	1.539701804	0.191721678
green	1.616541399	0.747186807
orange	2.067592522	0.701989482
red	1.668405937	0.401579404
blue-green	1.28489607	0.375258584
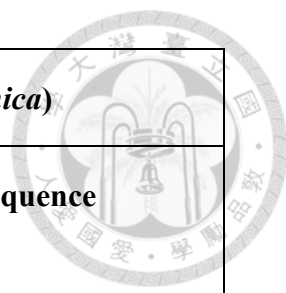
Table 4 Opsin candidate sequences (query: opsin, *Dugesia japonica*)		
Candidate sequences **in transcriptome database**	**e value**	**The most similar sequence** **in NCBI database**
NODE_35967_length_1434_ cov_10.143277_g19787_i0_pilon	1e-20	hypothetical protein LSAT2_007345, partial [*Lamellibrachia satsuma*]
NODE_27163_length_1870_ cov_8.094046_g14517_i0_pilon	9e-20	unnamed protein product [*Owenia fusiformis*]
NODE_24843_length_2016_ cov_12.511065_g13276_i0_pilon	7e-19	NKY receptor 1 [*Platynereis dumerilii*]
NODE_54299_length_863_ cov_4.878481_g33820_i0_pilon	7e-18	unnamed protein product [*Owenia fusiformis*]

Table 5 Cryptochrome candidate sequences

(query: cryptochrome, *Drosophila melanogaster*)

Candidate sequences in transcriptome database	e value	The most similar sequence in NCBI database
NODE_111686_length_359_ cov_2.643357_g89954_i0_pilon	2e-12	unnamed protein product, partial [*Rotaria magnacalcarata*]
NODE_88903_length_462_ cov_2.149100_g67176_i0_pilon	3e-12	DASH family cryptochrome [*Bacteroidetes bacterium*]
NODE_60414_length_750_ cov_2.704579_g39340_i0_pilon	6e-07	unnamed protein product [*Adineta ricciae*]

Table 6 BLUF photoreceptor candidate sequences

(query: bluF, *Escherichia coli*)

Candidate sequences in transcriptome database	e value	The most similar sequence in NCBI database
NODE_67319_length_652_ cov_3.875648_g45890_i0_pilon	1.2	BLUF domain-containing protein [*Aestuariicella hydrocarbonica*]
NODE_27549_length_1845_ cov_162.724605_g14730_i0_pilon	5.9	cytochrome b561 domain-containing protein 2-like [*Styela clava*]
NODE_30220_length_1700_ cov_5.256915_g16264_i0_pilon	6.5	cytochrome P450 7A1-like [*Haliotis rufescens*]

Table 7 LOV domain containing candidate sequences (query: LOV domain sequence, *Arabidopsis thaliana*)		
Candidate sequences in transcriptome database	**e value**	**The most similar sequence in NCBI database**
NODE_31779_length_1623_ cov_5.182581_g17174_i0_pilon	2e-30	hypothetical protein BJ166DRAFT_465879 [*Pestalotiopsis sp.* NC0098]
NODE_84275_length_492_ cov_3.023866_g62561_i0_pilon	3e-27	SAM domain (Sterile alpha motif) domain containing protein [*Acanthamoeba castellanii* str. Neff]
NODE_73080_length_588_ cov_3.258252_g51497_i0_pilon	1e-26	putative LOV domain-containing protein [*Fontinalis antipyretica*]
NODE_95302_length_426_ cov_3.158640_g73570_i0_pilon	2e-25	SAM domain (Sterile alpha motif) domain containing protein [*Acanthamoeba castellanii* str. Neff]
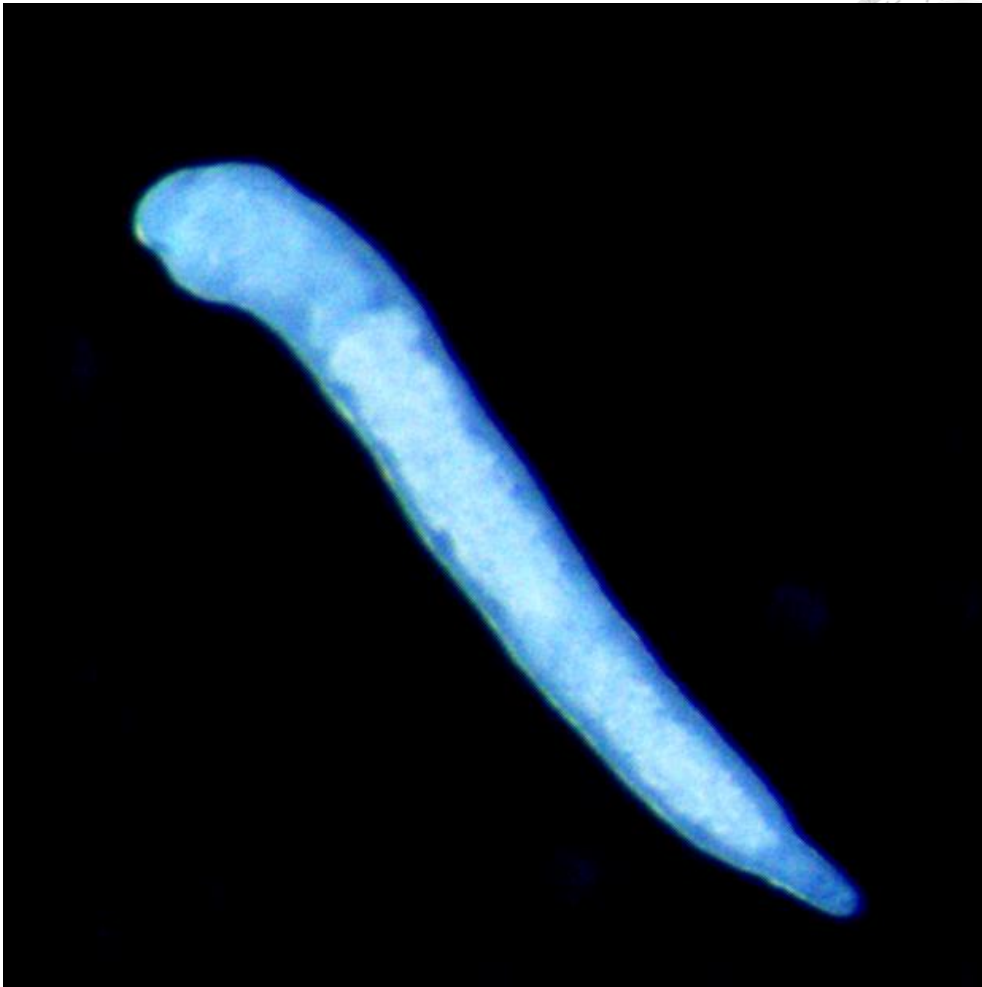
Fig. 1 The morphology of *S. grande.*
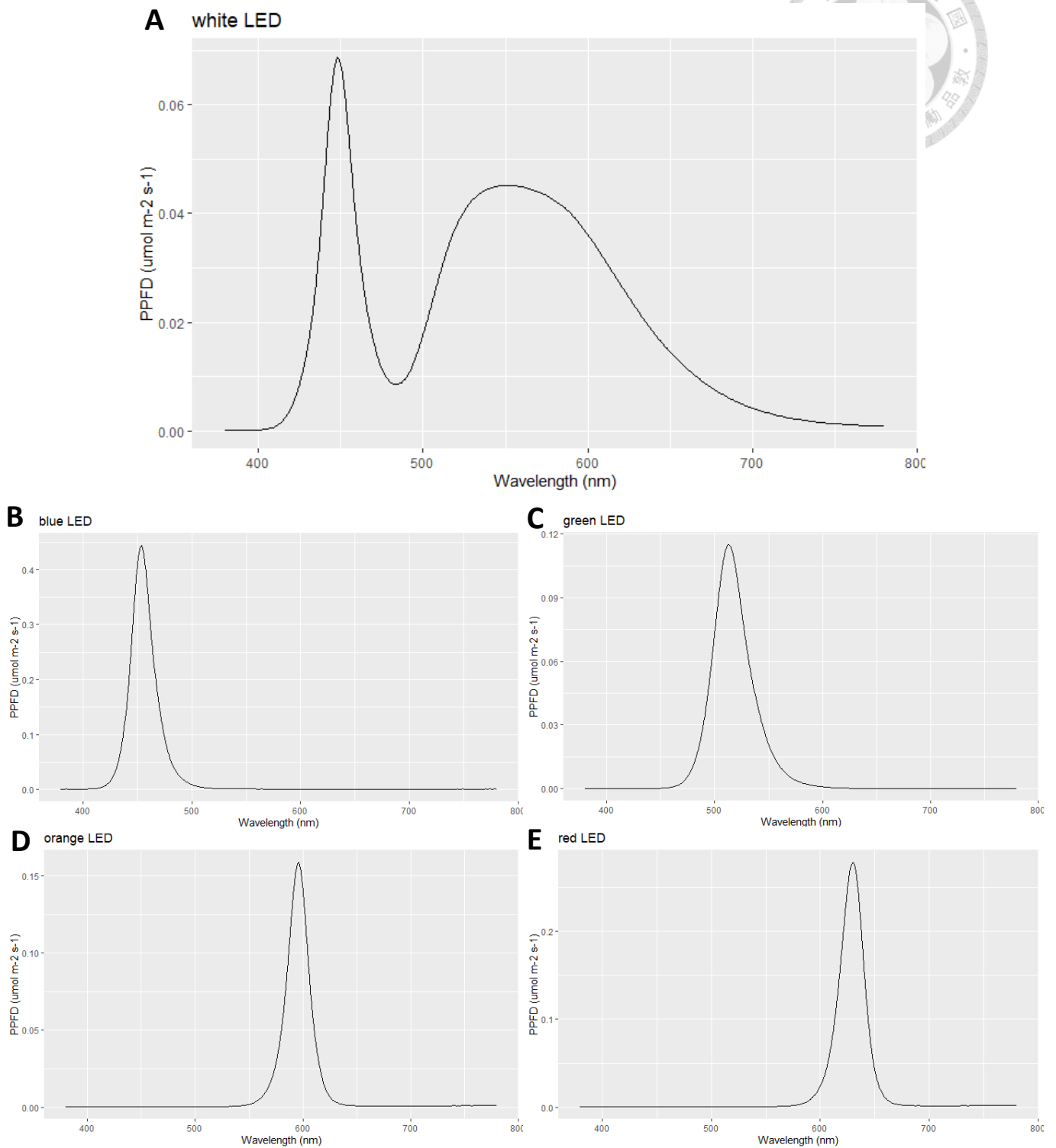
Fig. 2 The intensity of the light sources in different wavelength

(A) White LED light. (B) Blue LED light (peak = 454 nm). (C) Green LED light (peak = 514 nm). (D) Orange LED light (peak = 594 nm). (E) Red LED light (peak = 629 nm).
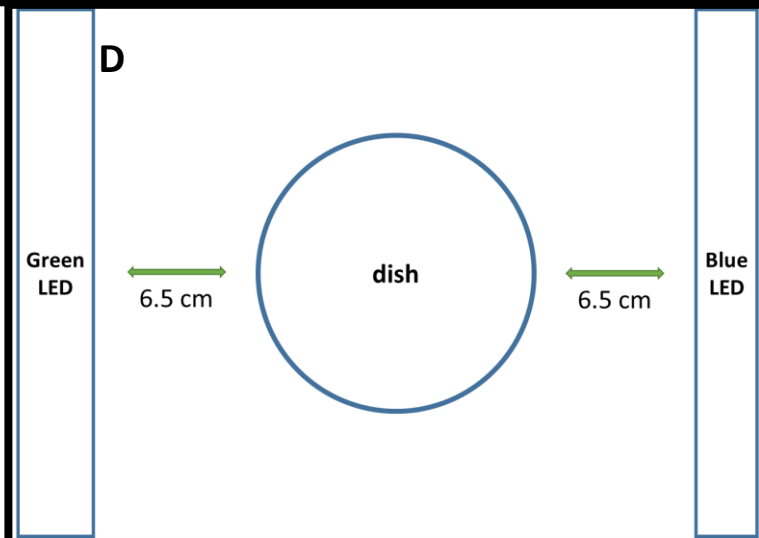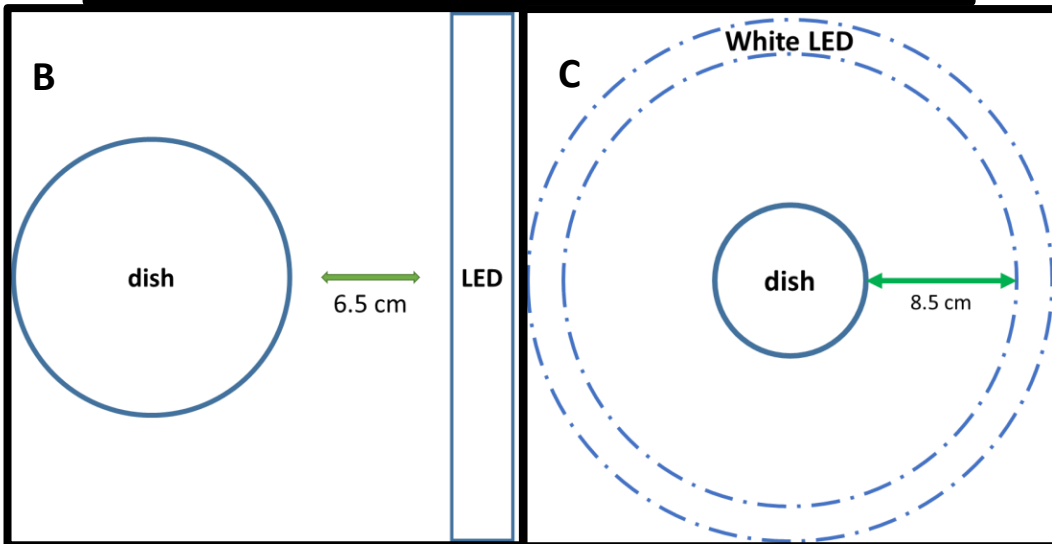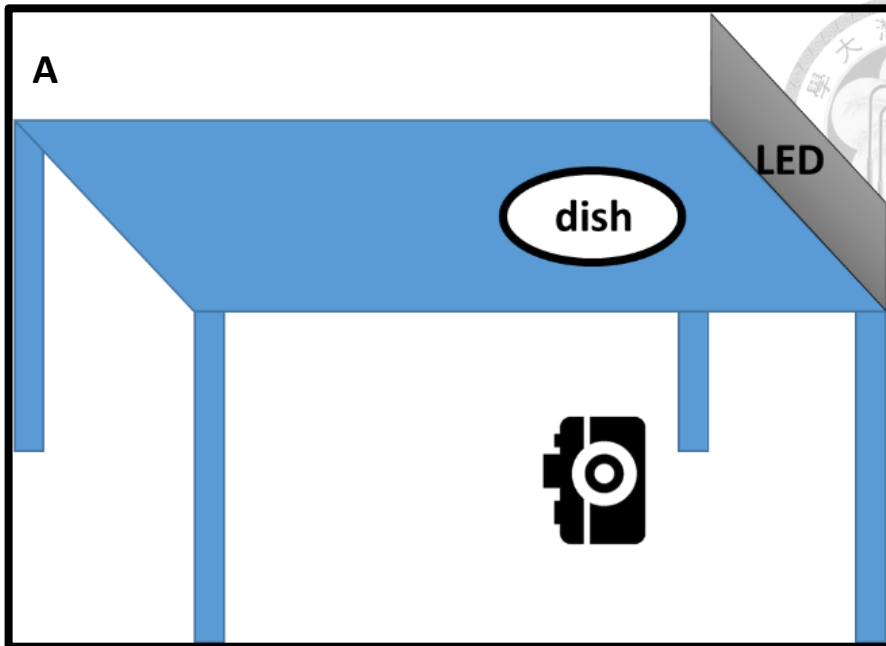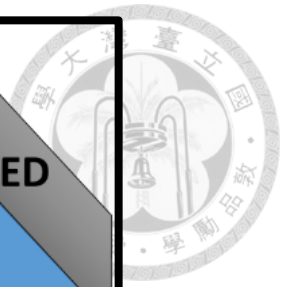
Fig. 3 The experimental setup of phototactic response assays

(A) The petri dish was placed on a black plastic board with a hole whose size was identical to the dish. The board was put on a platform, and a camera was under the testing dish. A LED strip was set in a straight form for most experiments. (B) The LED strip was set 6.5 cm away from the petri dish. (C) To eliminate a light gradient, the white LED strip was placed in circle around the dish. The distance between the dish and the LED strip was 8.5 cm. (D) A blue and a green LED strips were placed on the opposite sides of dish.
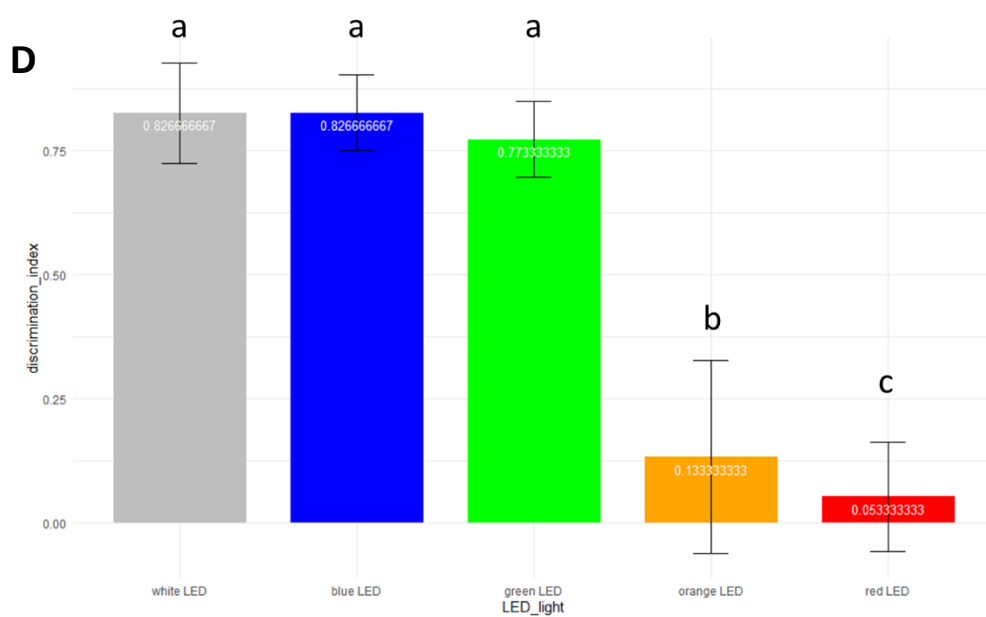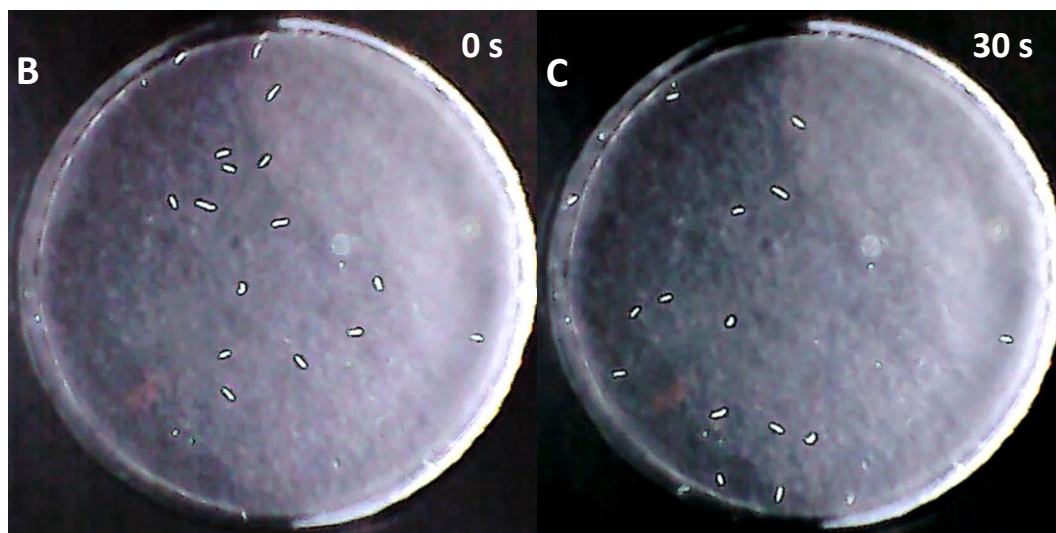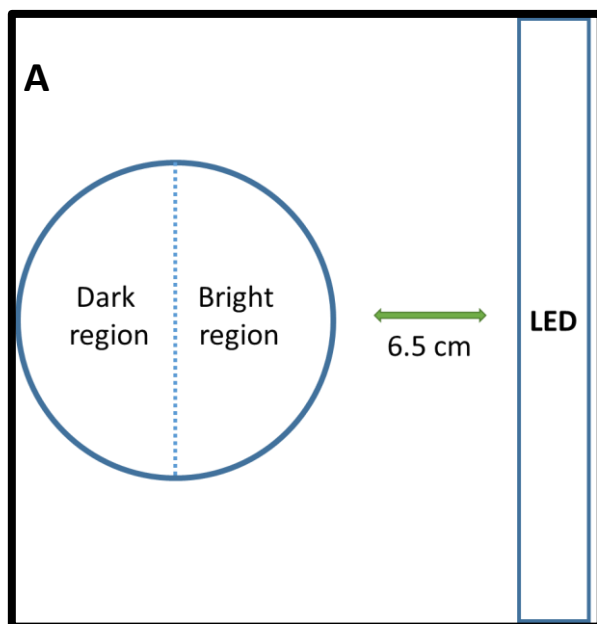
Fig. 4 The region discrimination assay and the discrimination indexes

(A) The petri dish was split into two parts. The one which was near the LED light was called the bright region, and the other was the dark region. (B) Distribution of worms when the white LED light just turned on (0 s). (C) Distribution of worms which were exposed to light for 30 seconds. (D) The discrimination indexes of five different lights. DI = (worms in the dark region – worms in the bright region) / total number of worms. (n = 5, 50 worms in each assay)

G white

H control 1

I control 2
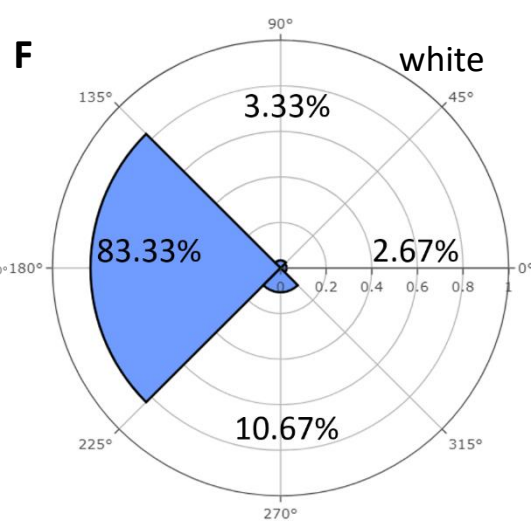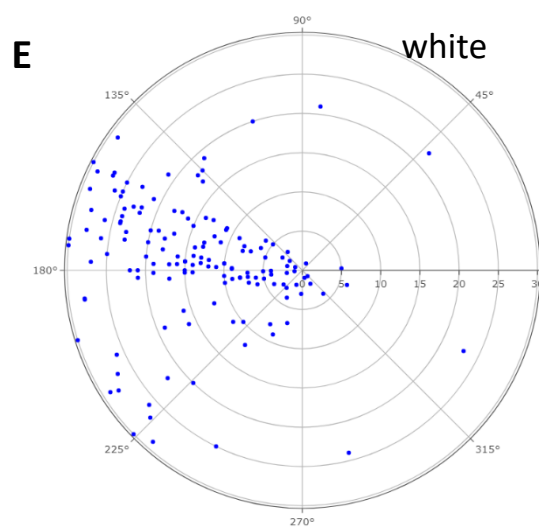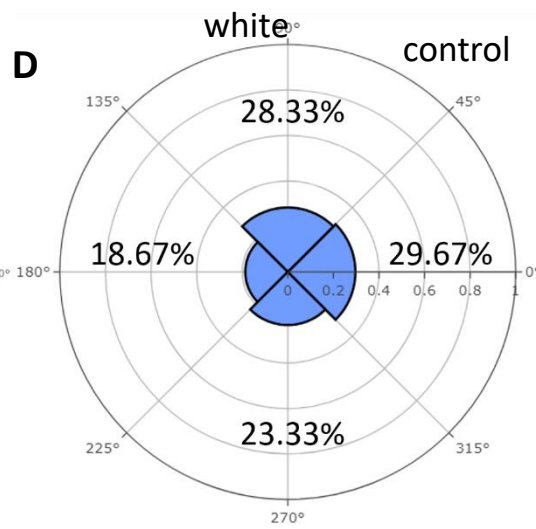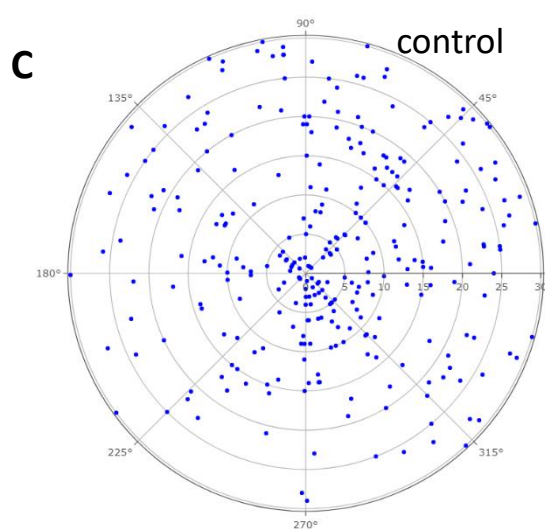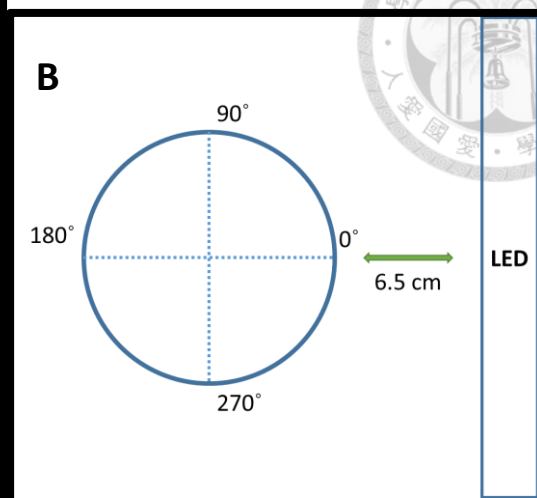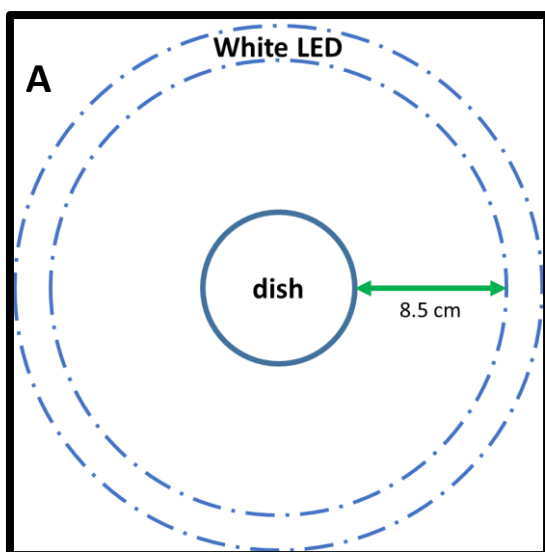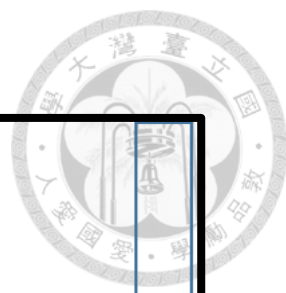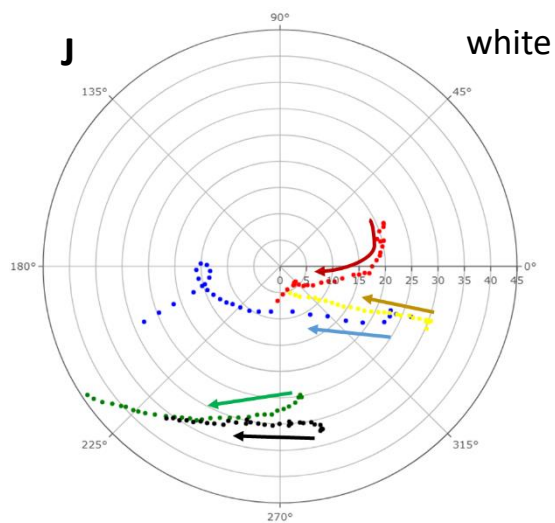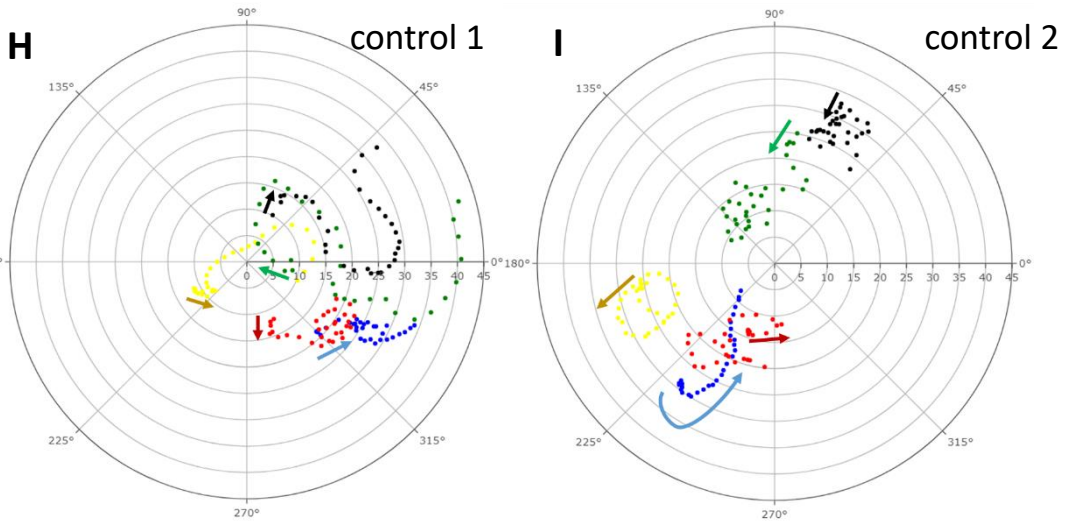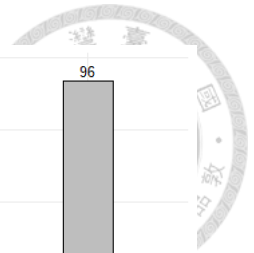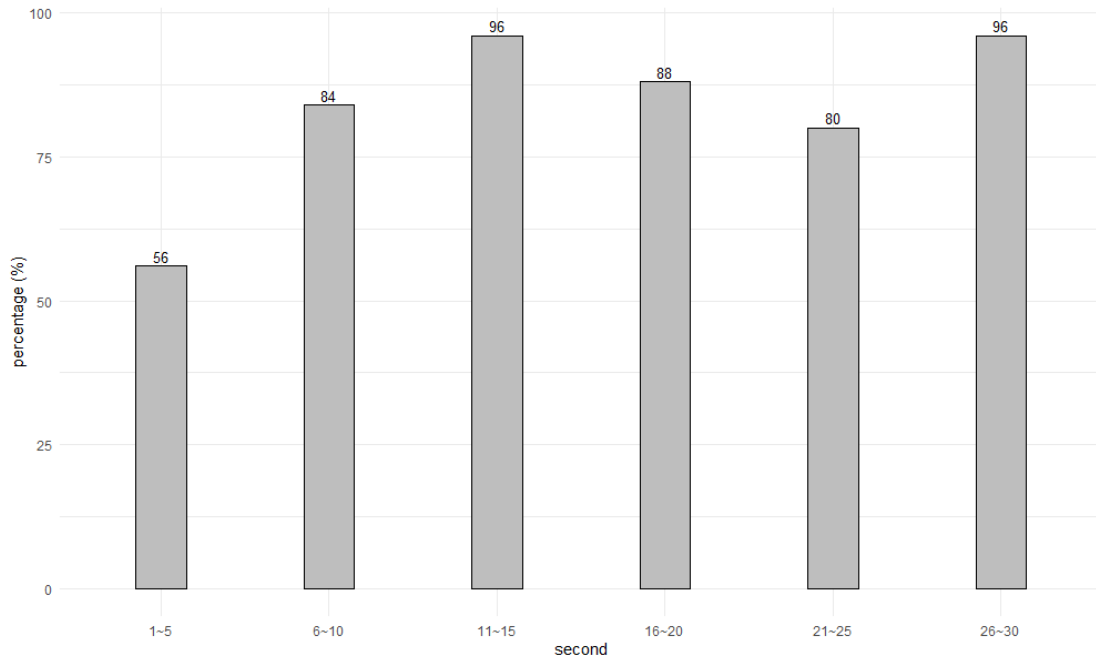
J white

Fig. 5 The directional phototactic response assay

(A) To eliminate a light gradient, the white LED strip was placed in circle around the dish. The distance between the dish and the LED strip was 8.5 cm. (B) The LED strip was set 6.5 cm away from the petri dish. The angles of the dish were defined so that the analysis of the movement could be easier. The LED light was from 0°. (C) (E) Polar charts of the head directions. The angles of the head directions were recorded once per second (control: n = 10; white: n = 5). 30 seconds of movements were recorded. The radius in this plot represents total time of the experiment (30 s). (D) (F) The percentage of four different angle groups: 0° (315° ~ 45°), 90° (45° ~ 135°), 180° (135° ~ 225°), 270° (225° ~315°). (G) The percentage of 180° (135° ~ 225°) groups with exposure to white light in different time frames. (H) (I) (J) The coordinates of the worms were recorded once per second (n = 5 in each assay). 30 seconds of movements were recorded. The radius in this plot represents the distance from the center of the dish (the diameter of the dish is 90 mm). The arrow represents the moving direction from the start.
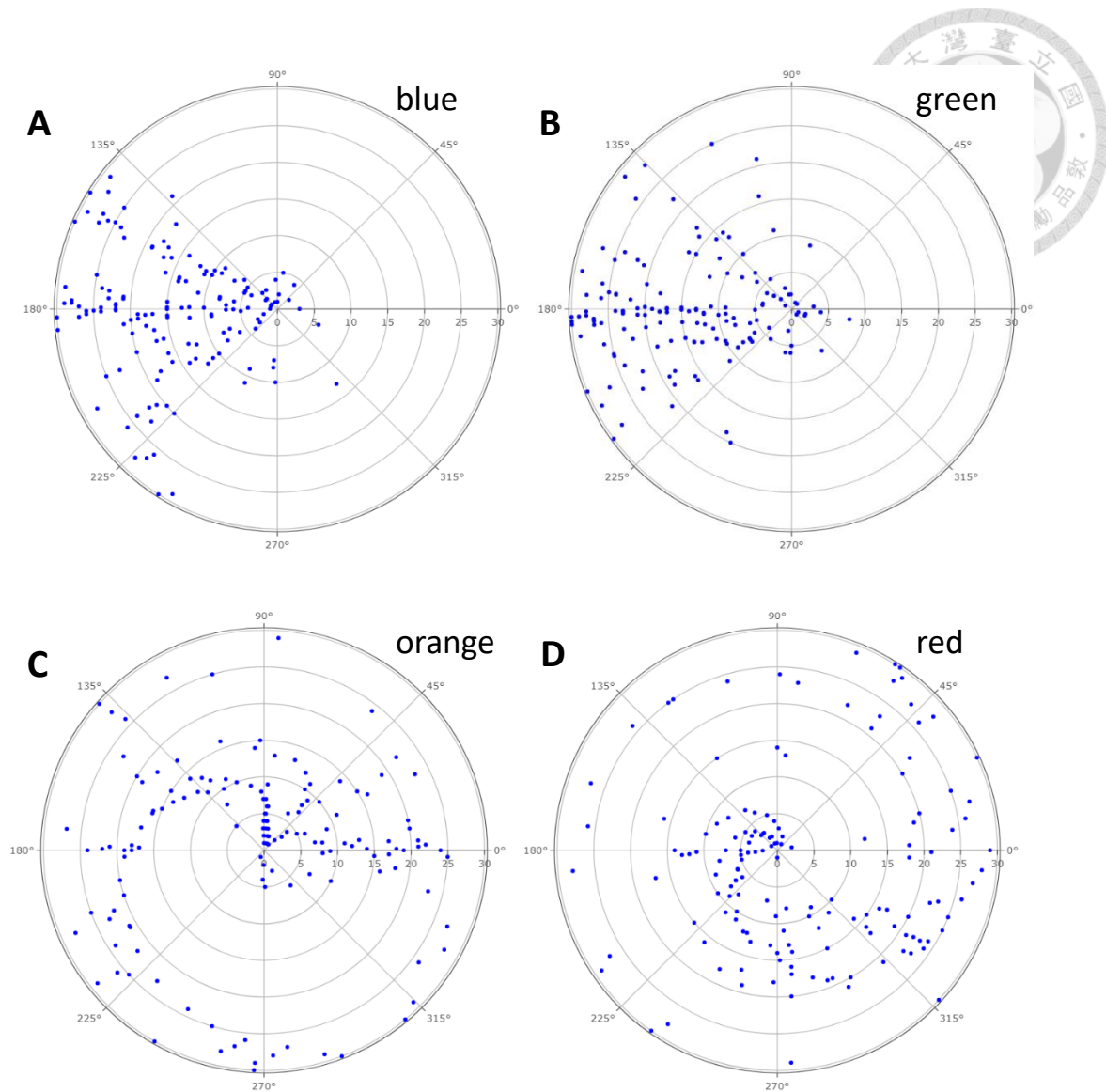
Fig. 6 The directional phototactic response assay for four different wavelengths of light.

The experimental setup was the same as white light assays (n = 5 in each assay). 30 seconds of movements were recorded. The radius in this plot represents total time of the experiment (30 s). (A) Blue LED light (peak = 454 nm). (B) Green LED light (peak = 514 nm). (C) Orange LED light (peak = 594 nm). (D) Red LED light (peak = 629 nm).
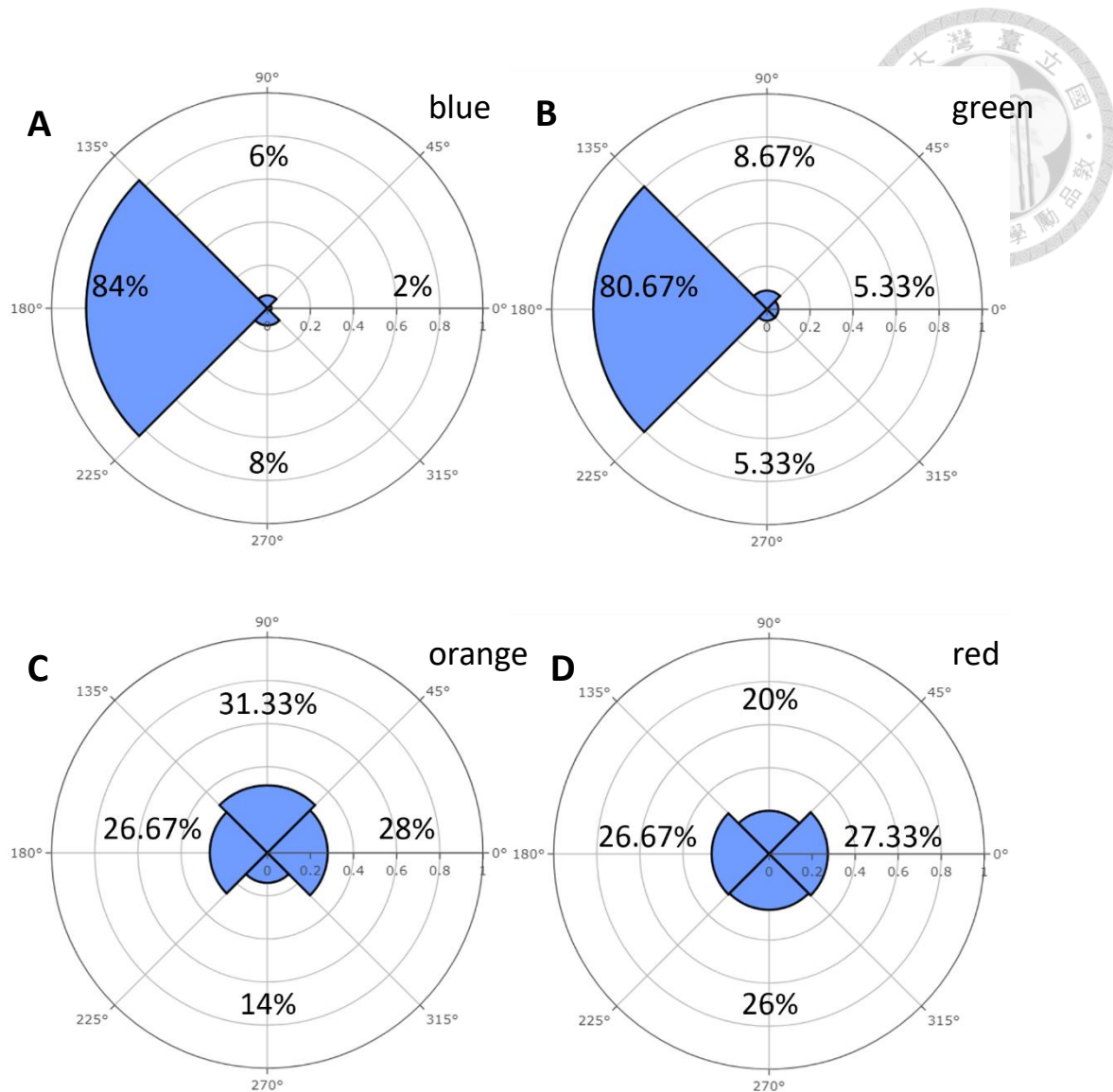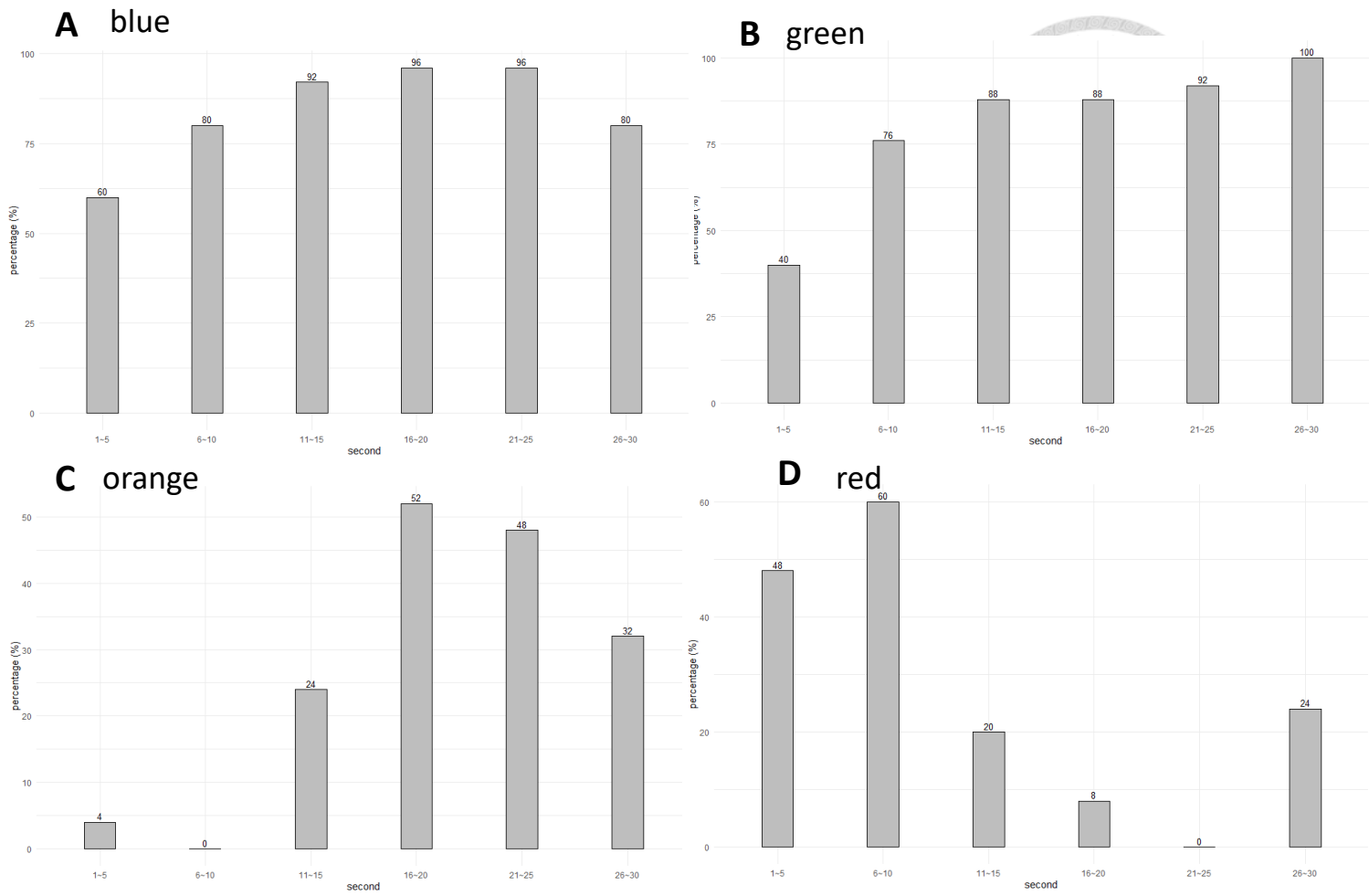
Fig. 7 The percentage of four different angle groups for four different wavelengths of light.

The angle ranges were separated into four groups. 0° (315° ~ 45°), 90° (45° ~ 135°), 180° (135° ~ 225°), 270° (225° ~ 315°).　(A) Blue LED light (peak = 454 nm). (B) Green LED light (peak = 514 nm). (C) Orange LED light (peak = 594 nm). (D) Red LED light (peak = 629 nm).

Fig. 8 The percentage of 180° (135° ~ 225°) groups for distinct lights in different time frames.

(A) Blue LED light (peak = 454 nm). (B) Green LED light (peak = 514 nm). (C) Orange LED light (peak = 594 nm). (D) Red LED light (peak = 629 nm)
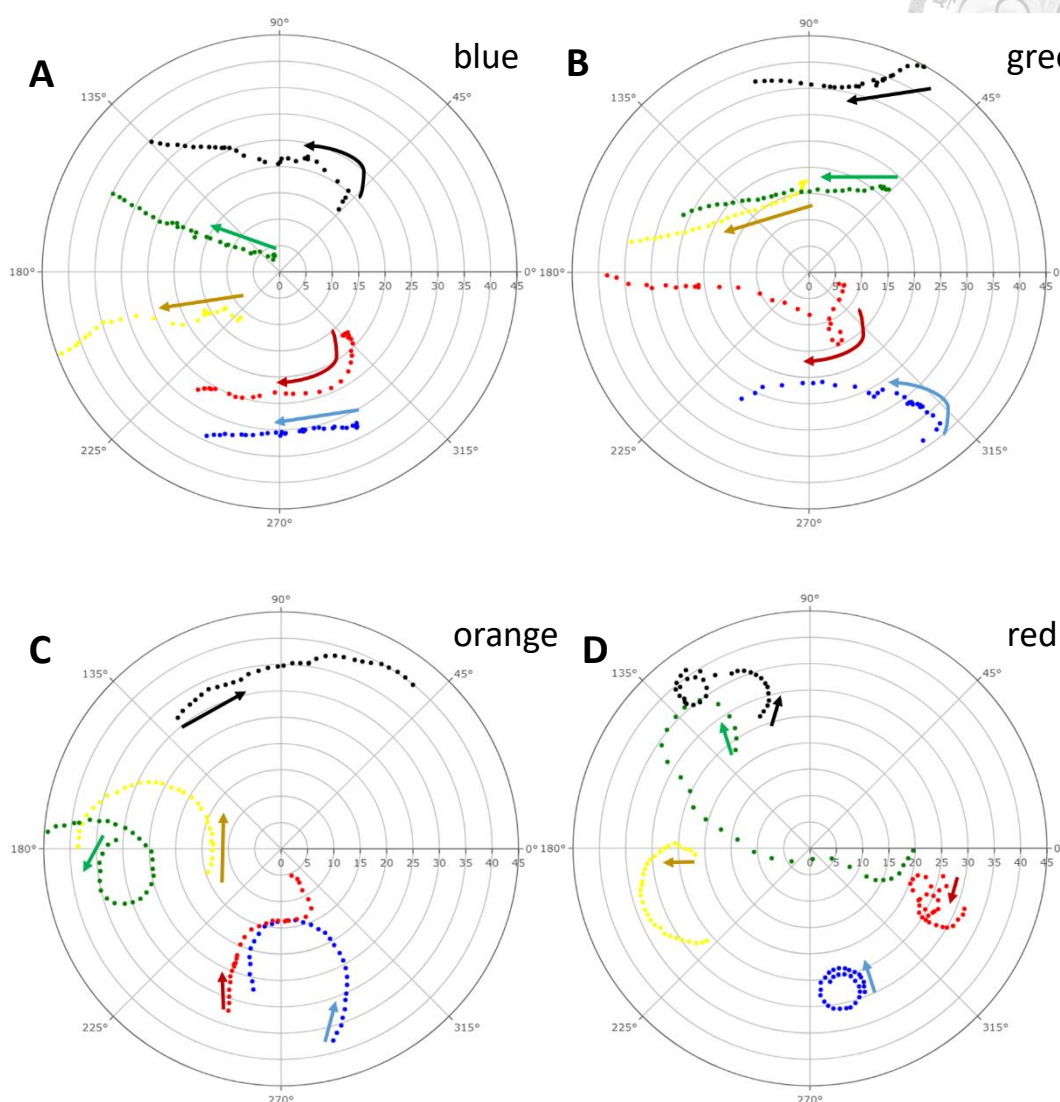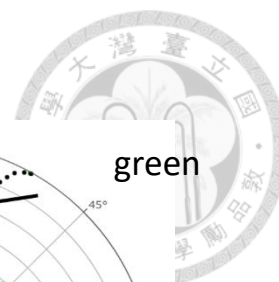
Fig. 9 The trajectories of the worms for four different wavelengths of light.

The coordinates of the worms were recorded once per second (n = 5 in each assay). 30

seconds of movements were recorded. The radius in this plot represents the distance from

the center of the dish (the diameter of the dish is 90 mm).

(A) Blue LED light (peak = 454 nm). (B) Green LED light (peak = 514 nm). (C) Orange

LED light (peak = 594 nm). (D) Red LED light (peak = 629 nm)
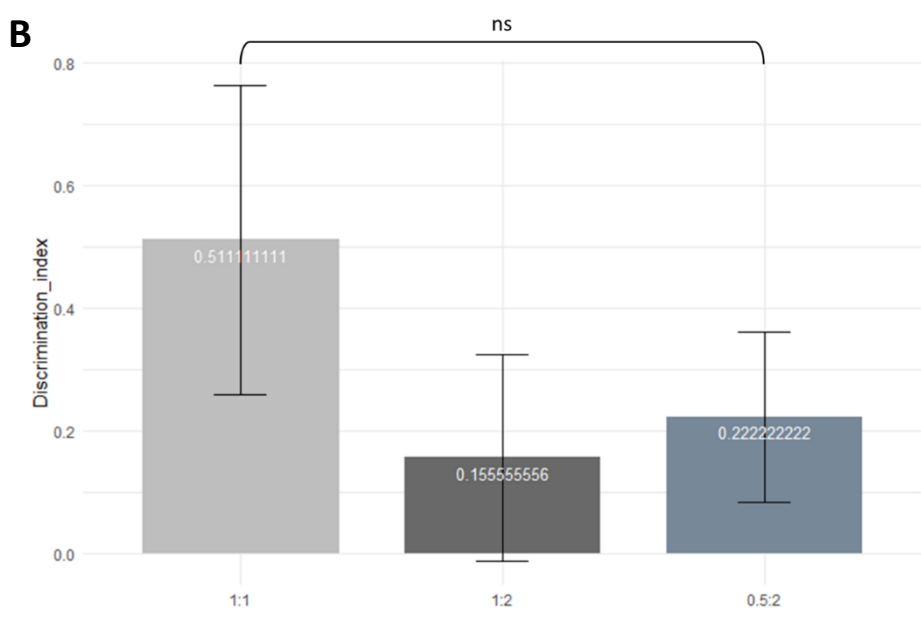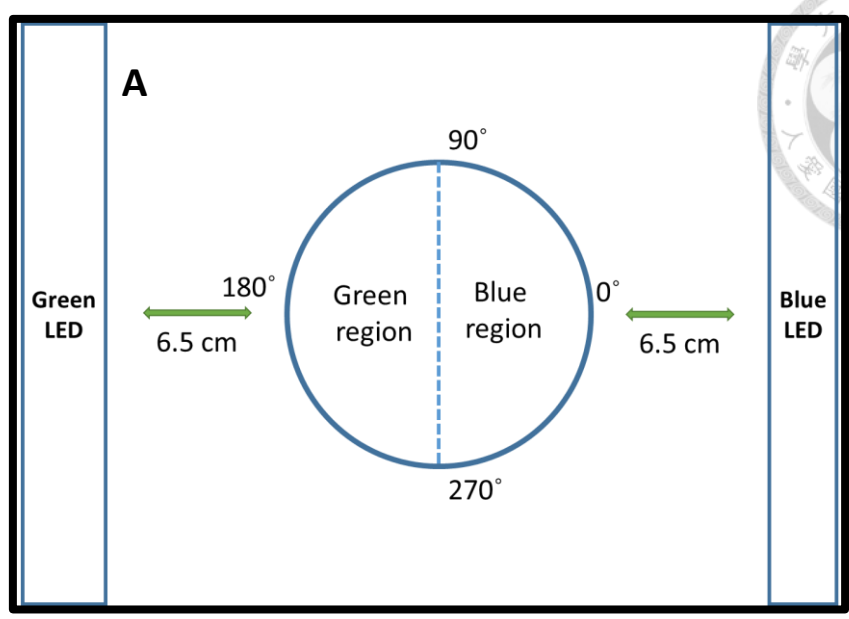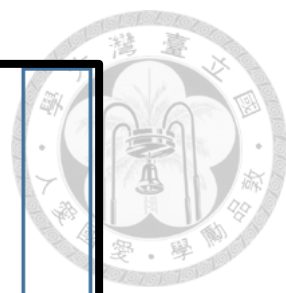
Fig. 10 The wavelength choosing assay and the discrimination indexes with different arrangement.
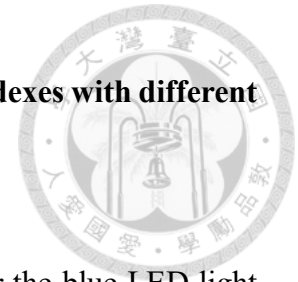
(A) The petri dish was split into two parts. The one which was near the blue LED light was called the blue region, and the other which was near the green LED light was called the green region. (B) The discrimination indexes of five different lights. DI = (worms in the green region – worms in the blue region) / total number of worms. These data had no statistical significance. (n = 3, 30 worms in each assay)
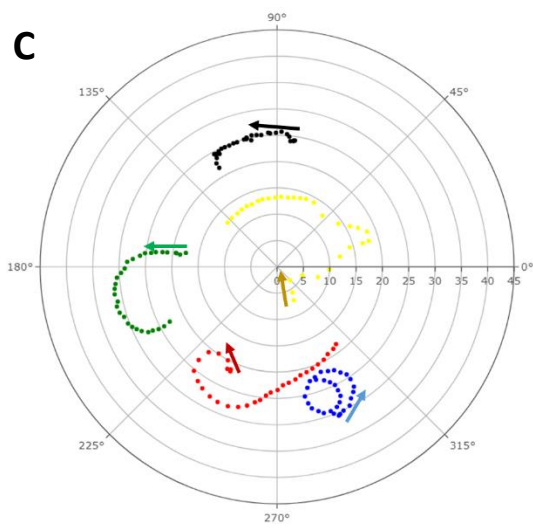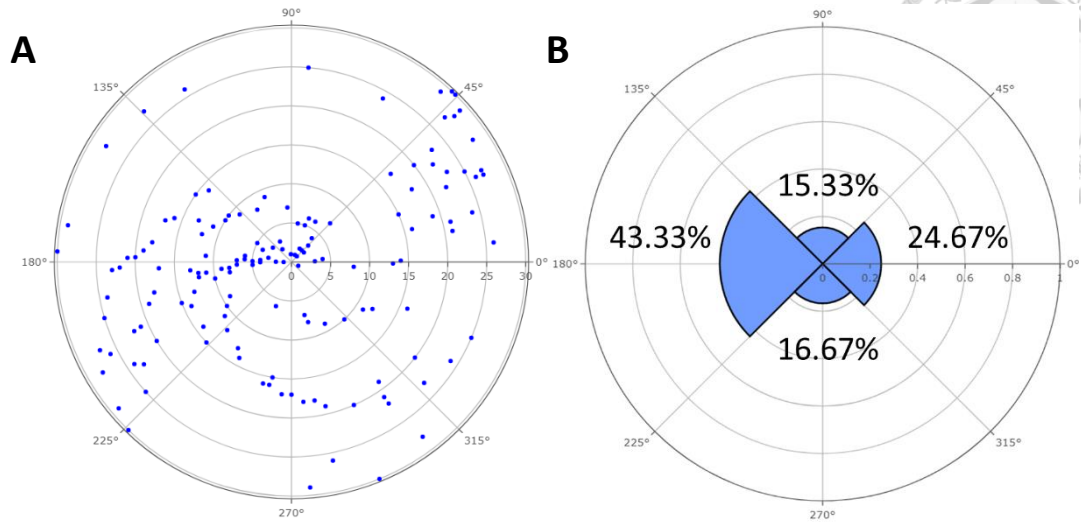
Fig. 11 Determination of the moving directions in the wavelength choosing assay.

The blue LED light was from 0˚, and the green LED light was from 180˚. The intensity of two lights were identical. (A) The experimental setup was the same as white light assays (n = 5). 30 seconds of movements were recorded. The radius in this plot represents total time of the experiment (30 s). (B) The percentage of four different angle groups. (C) The coordinates of the worms were recorded once per second (n = 5 in each assay). 30 seconds of movements were recorded. The radius in this plot represents the distance from the center of the dish (the diameter of the dish is 90 mm).
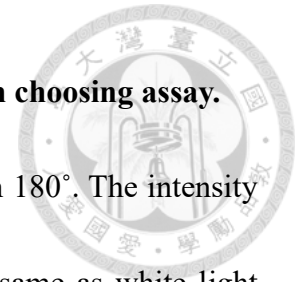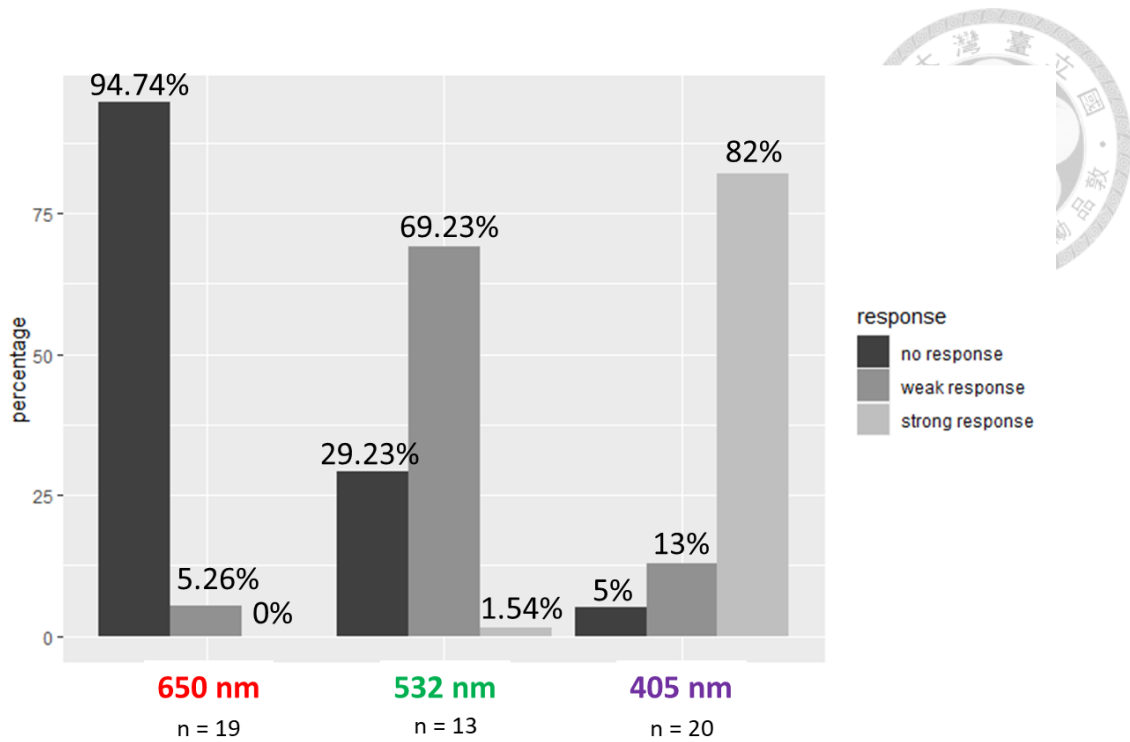
Fig. 12 The laser irradiating test.

Three different responses were defined. The worms were exposed to three different

wavelengths of light. The data was collected from the first 5 responses for each worm.

(Red, 664 nm, n = 19; Green, 539 nm, n = 13; Violet, 404 nm, n = 20)
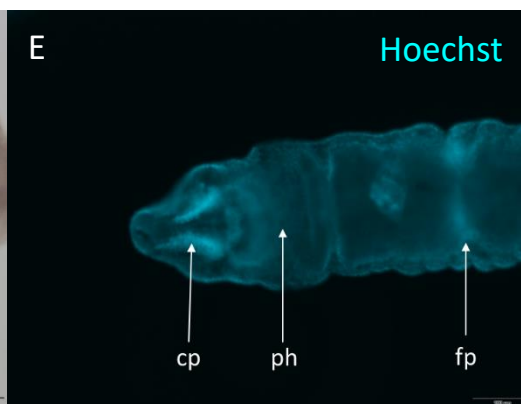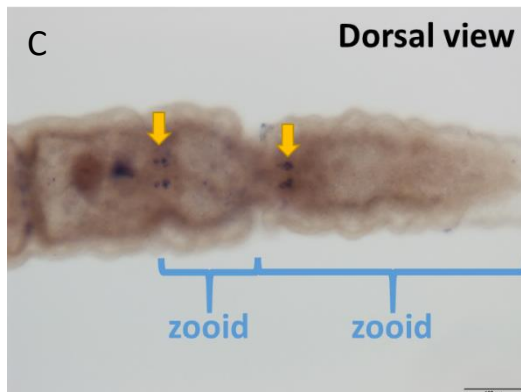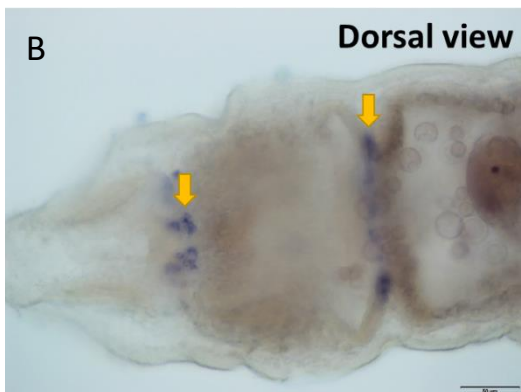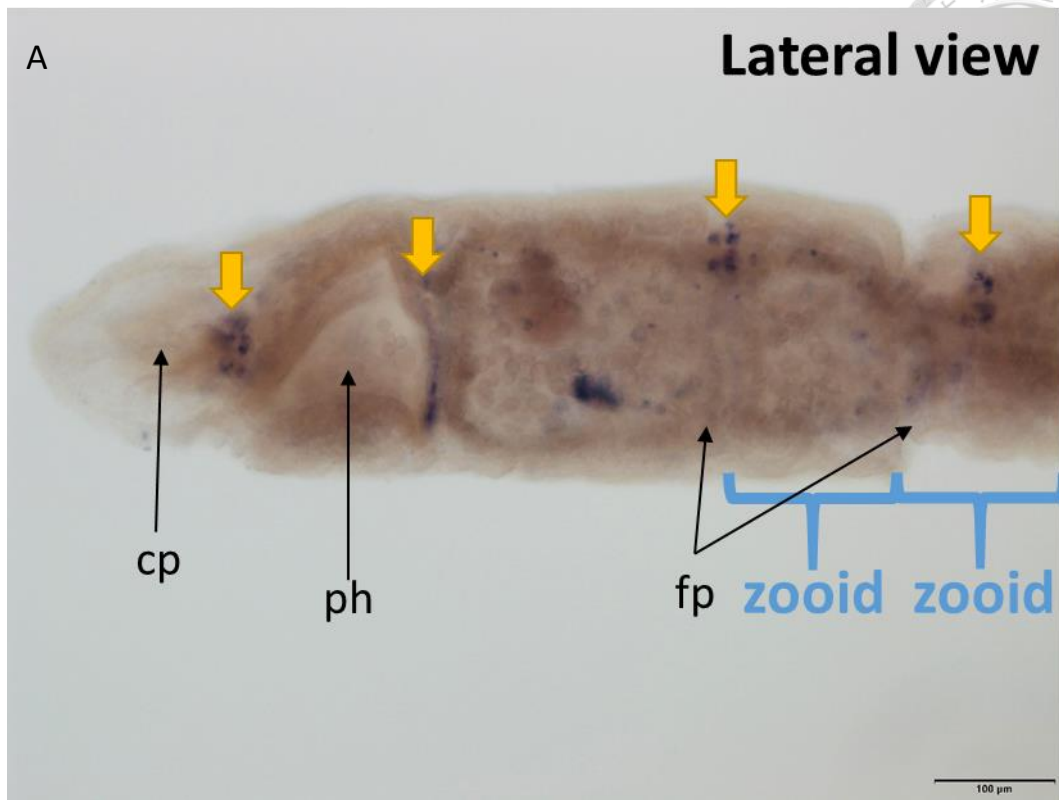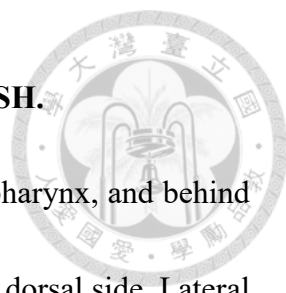
Fig. 13 The cell bodies which express *ChAT* were revealed by WISH.

(A) The cell bodies are restricted in the cerebral ganglion, near the pharynx, and behind

fission plans. The labeled cells behind fission plans are located at the dorsal side. Lateral

view.   (B) The labeled cells near the pharynx seem to surround the pharynx, and the cells

in the cerebral ganglion seem to be four clusters. Dorsal view. (C) The labeled cells behind

fission plans are observed that there are also four groups of cells. They may develop into

new cerebral ganglia in new organisms. Dorsal view. (D) (E) To recognize whether the

labeled structures are cell bodies, the Hoechst staining was performed. Dorsal view.

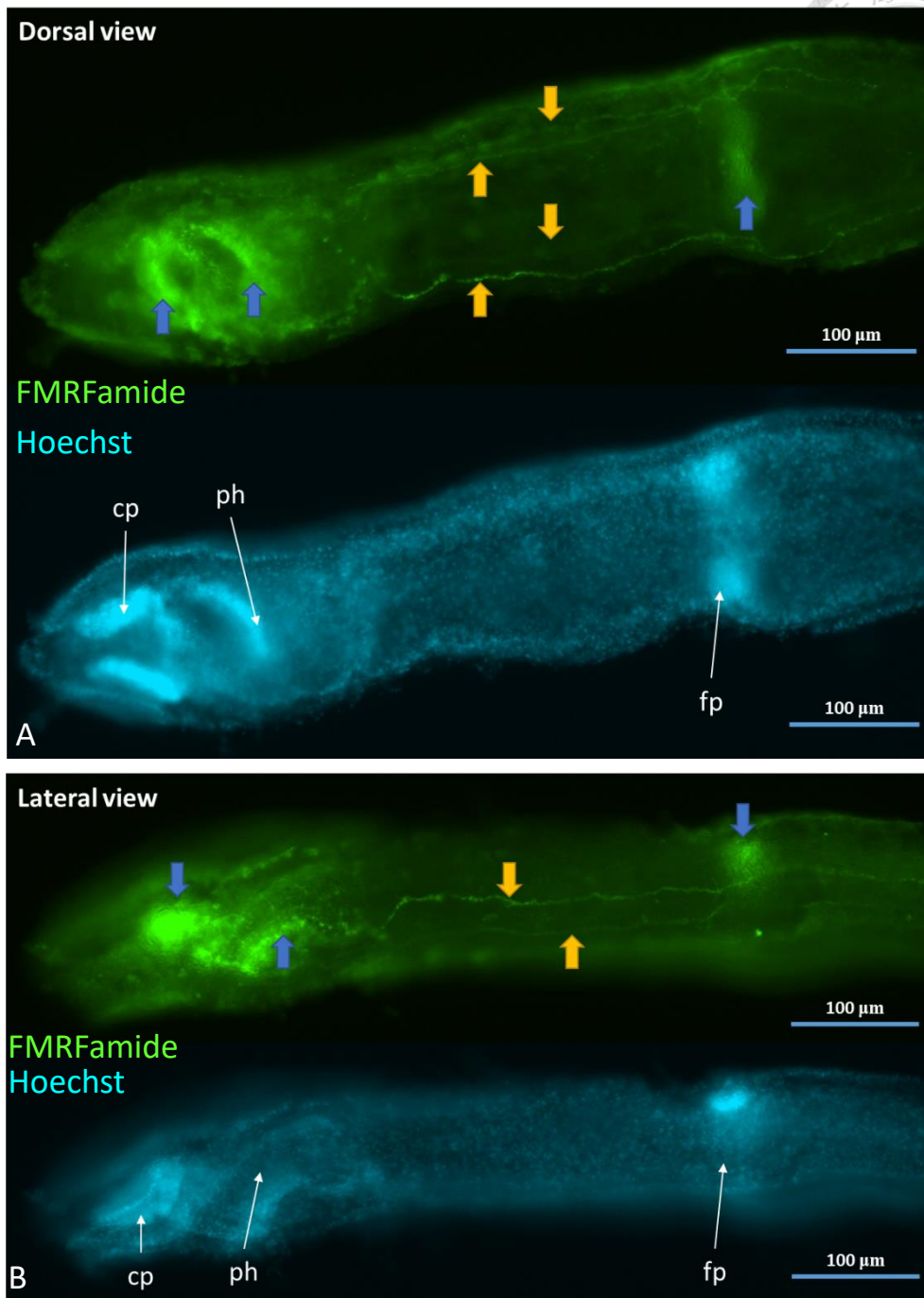cp: ciliated pits, ph: pharynx, fp: fission plan

Dorsal view

FMRFamide
Hoechst

cp   ph

fp

100 µm

100 µm

A

Lateral view

FMRFamide
Hoechst

100 µm

B   cp   ph   fp   100 µm

Fig. 14 The FMRFamide-like immunoreactive (-lir) cells and fibers are revealed by immunostaining.

The blue arrows point at the FMRFamide-lir structures which are hypothesized to be cell bodies. These regions are similar to the regions which express *ChAT* in the previous experiment. The yellow arrows point at the FMRFamide-lir structures which are believed to be ventral nerves. Four ventral nerves can be observed.

(A)Dorsal view. (B) Lateral view.
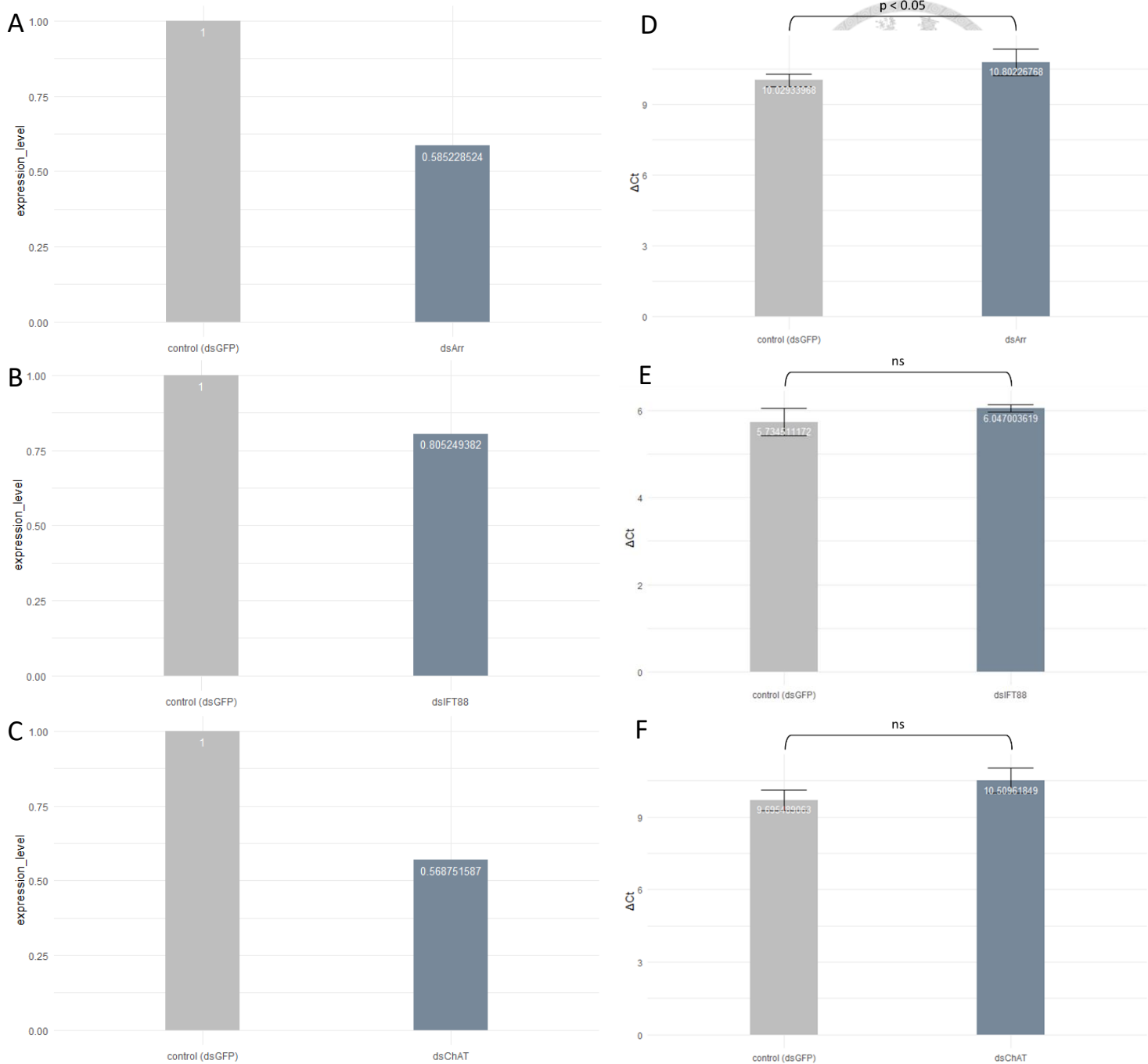
cp: ciliated pits, ph: pharynx, fp: fission plan

Fig. 15 The ΔCt and expression levels of RNA interference.

ΔCt = Ct (gene of interest) – Ct (*β-actin*). ΔΔCt = ΔCt (dsRNA group) – ΔCt (ds*GFP*).

Expression level = 2^(-ΔΔCt). (A) (B) The ΔCt and expression level of *Arr*. (C) (D) The

ΔCt and expression level of *IFT88*. (E) (F) The ΔCt and expression level of *ChAT*.

Video

Vedio 1 The phototactic response assay (the white LED group)

https://youtu.be/qYWfBNmw-4g

Vedio 2 The phototactic response assay (the control group)

https://youtu.be/scPUxAepe14

Vedio 3 The phototactic response assay (the blue LED group)

https://youtu.be/G7VFe3dhE28

Vedio 4 The phototactic response assay (the green LED group)

https://youtu.be/AngO1FNoJOw

Vedio 5 The phototactic response assay (the orange LED group)

https://youtu.be/FcezPku6eBg

Vedio 6 The phototactic response assay (the red LED group)

https://youtu.be/UR2nZeG4OlY

Vedio 7 The Wavelength Choosing Assay (B:G = 1:1)

https://youtu.be/7N_pSxrU9M0

Vedio 8 The Wavelength Choosing Assay (B:G = 1:2)

https://youtu.be/ZImKMN2df5E

Vedio 9 The Wavelength Choosing Assay (B:G = 0.5:2)

https://youtu.be/dqhrpaEvYcs

Vedio 10 The laser irradiating test (violet)

https://youtu.be/KadyVY6MydM

Vedio 11 The laser irradiating test (green)

https://youtu.be/ULcGcV8x-RY

Vedio 12 The laser irradiating test (red)

https://youtu.be/shZBfqOOh1Y